

**UNIVERSITI MALAYSIA PAHANG**

**BORANG PENGESAHAN STATUS TESIS**

**JUDUL: EXPERIMENTAL AND SIMULATION STUDY ON THE EFFECT OF INNER SPAN IN A FOUR-POINT BENDING TEST (4PB)**

**SESI PENGAJIAN: 2011/2012**

Saya, **MUHAMMAD ZAKI B CHE MD NOR (900326-03-5259)**  
(HURUF BESAR)

mengaku membenarkan tesis (Sarjana Muda / ~~Sarjana / Doktor Falsafah~~)\* ini disimpan di perpustakaan dengan syarat-syarat kegunaan seperti berikut:

1. Tesis ini adalah hakmilik Universiti Malaysia Pahang (UMP).
2. Perpustakaan dibenarkan membuat salinan untuk tujuan pengajian sahaja.
3. Perpustakaan dibenarkan membuat salinan tesis ini sebagai bahan pertukaran antara institusi pengajian tinggi.
4. \*\*Sila tandakan (✓)

**SULIT**

(Mengandungi maklumat yang berdarjah keselamatan atau kepentingan Malaysia seperti yang termaktub di dalam AKTA RAHSIA RASMI 1972)

**TERHAD**

(Mengandungi maklumat TERHAD yang telah ditentukan oleh organisasi / badan di mana penyelidikan dijalankan)

**TIDAK TERHAD**

Disahkan oleh:



\_\_\_\_\_  
(TANDATANGAN PENULIS)

\_\_\_\_\_  
(TANDATANGAN PENYELIA)

Alamat Tetap:  
**LOT 1843 KG CHABANG 4 TENDONG**  
**17030 PASIR MAS**  
**KELANTAN**  
Tarikh: **25 JUN 2012**

**MOHD ZAIDI BIN SIDEK**

(Nama Penvelia)

Tarikh: **25 JUN 2012**

CATATAN: \* Potong yang tidak berkenaan.

\*\* Jika tesis ini SULIT atau TERHAD, sila lampirkan surat daripada pihak berkuasa/organisasi berkenaan dengan menyatakan sekali tempoh tesis ini perlu dikelaskan sebagai SULIT atau TERHAD.

- ◆ Tesis dimaksudkan sebagai tesis bagi Ijazah Doktor Falsafah dan Sarjana secara Penyelidikan, atau disertasi bagi pengajian secara kerja kursus dan penyelidikan, atau Laporan Projek Sarjana Muda (PSM).

EXPERIMENTAL AND SIMULATION STUDY ON THE EFFECT OF INNER SPAN  
IN A FOUR-POINT BENDING TEST (4PB)

MUHAMMAD ZAKI BIN CHE MD NOR

Report submitted in partial fulfilment of the requirements  
for the award of the degree of  
Bachelor of Mechanical Engineering

Faculty of Mechanical Engineering  
UNIVERSITI MALAYSIA PAHANG

JUNE 2012

**UNIVERSITI MALAYSIA PAHANG**  
**FACULTY OF MECHANICAL ENGINEERING**

I certify that the project entitled “*Experimental and simulation study on the effect of inner span in a four-point bending test (4PB)*” is written by *Muhammad Zaki Bin Che Md Nor*. I have examined the final copy of this project and in our opinion, it is fully adequate in terms of scope and quality for the award of the degree of Bachelor of Engineering. I herewith recommend that it be accepted in partial fulfilment of the requirements for the degree of Bachelor of Mechanical Engineering.

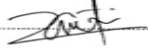
*Nasrul Azuan Bin Alang*

Examiner

Signature

### SUPERVISOR'S DECLARATION

I hereby declare that I have checked this project report and in our opinion this project is satisfactory in terms of scope and quality for the award of the degree of Bachelor of Mechanical Engineering with "specialization".

Signature :   
Name of Supervisor : MR MOHD ZAIDI BIN SIDEK  
Position : FACULTY OF MECHANICAL ENGINEERING LECTURER  
Date : 25 JUNE 2012

## STUDENT'S DECLARATION

I hereby declare that the work in this report is my own except for quotations and summaries which have been duly acknowledged. The report has not been accepted for any degree and is not concurrently submitted for award of other degree.

Signature :

Name : MUHAMMAD ZAKI BIN CHE MD NOR

ID Number : MA08131

Date : 25 JUNE 201

## ACKNOWLEDGEMENTS

I would like to thank all people who have helped and inspired me during completed this studies. I especially want to thank my supervisor, Mr Mohd Zaidi Bin Sidek, for his guidance during completed this project. His perpetual energy and enthusiasm in supervising had motivated his entire student, including me. In addition, he was always accessible and willing to help her students with their project. As a result, this project can be completed.

All of my friends at the Universiti Malaysia Pahang made it a convenient place to study. In particular, I would like to thank my lab mates, Mohd Syazwan B Zulkipli, Abdul Zarif Bin Abdul Malek, Mohd Shahril Bin Mohd Hassan, Mohd Adzlan Bin Mohd Azmi, Mohd Jaafar Bin Mohd Nor, and all of the staff of the Mechanical Engineering Department, UMP who helped me in many ways.

I acknowledge my sincere indebtedness and gratitude to my lovely mother, Nafisah Binti Yaacob for her sacrifice and support throughout my life. My deepest gratitude goes to my family for their unflagging love and support throughout my life; this dissertation is simply impossible without them. Last but not least, thanks be to God for giving us living in this universe and provide us with all necessary things.

## ABSTRACT

The main aim of this study is to compare experimental four point bending test with finite element simulation. This study begins with a literature study. It was followed by design and fabrication of test equipment for four point bending test. This study begins with a preliminary design using Solidwork software and fabrication of a test equipment for four point bending test. This research work exposes student with many aspect of engineering work; design, fabrication and testing a product. The fabricated test rig consists of three main parts. Finite element evaluation is one of the methods in predicting the strain value in sheet metal bending. Predicting the strain value is sometimes used in areas of plastic deformation, which is the integral of the ratio of the incremental change in length to the instantaneous length of a plastically deformed. This thesis aims to evaluate the reliability of finite element method by comparing the results with experimental results. The effect of parameters such as length of displacement after bend also has been studied. Abaqus software has been used to simulate the bending process and the mechanical properties provided from the Solidwork data will be used to run the simulation. In the four-point bending experiment, the test rig was clamped on Shimadzu machine and the mild steel sheets was assembled with strain gauge before bend process was run. Strain value being measured with DasyLab software. The results from the experiment and simulation is slightly different for value of strain, which the simulation shows the value of strain higher than strain value that was get from the experiment. For the free force four-point bending, value length displacement after bend almost the same on the simulation and experimental. Finite element method can be used to make comparison since the pattern of the graphs are nearly the same and percentages of error are below 10 %. The further study on parameters that effected bending process will make the finite element method is important in the future.

## ABSTRAK

Tujuan utama kajian ini adalah untuk membandingkan eksperimen empat titik ujian lentur dengan kaedah simulasi. Kajian ini bermula dengan kajian sastera. Ia diikuti oleh reka bentuk dan pembikinan peralatan ujian bagi ujian lenturan empat titik. Kajian ini bermula dengan reka bentuk awal menggunakan perisian Solidwork dan fabrikasi peralatan ujian. Kerja-kerja penyelidikan ini mendedahkan pelajar dengan banyak aspek kerja-kerja kejuruteraan; reka bentuk, fabrikasi dan menguji sesuatu produk. Pelantar ujian yang direka terdiri daripada tiga bahagian utama. Kaedah analisis simulasi merupakan salah satu kaedah untuk meramal nilai terikan dalam pembengkokan kepingan logam. Ramalan nilai terikan kadang-kadang digunakan dalam bidang ubah bentuk plastik, yang penting nisbah perubahan pertambahan panjang panjang ketika plastik cacat. Laporan ini bertujuan untuk menilai kebolehan kaedah simulasi dengan membandingkan keputusan simulasi dengan keputusan eksperimen. Kesan parameter seperti panjang anjakan selepas selekoh juga dikaji. Perisian Abaqus telah digunakan untuk mensimulasikan proses lenturan dan sifat-sifat mekanik yang disediakan dalam data perisian Solidwork akan digunakan untuk menjalankan simulasi. Dalam eksperimen lentur empat mata, rig ujian telah dikepit pada mesin Shimadzu dan kunci keluli lembut telah dipasang dengan tolok terikan sebelum proses lenturan dijalankan. Nilai terikan diukur dengan menggunakan perisian DasyLab. Hasil dari eksperimen dan simulasi adalah sedikit berbeza untuk nilai terikan, di mana simulasi menunjukkan nilai ketegangan yang lebih tinggi daripada nilai terikan yang telah didapati dari eksperimen. Untuk tenaga bebas empat mata lenturan, nilai anjakan panjang selepas selekoh yang hampir sama pada simulasi dan eksperimen. Kaedah simulasi boleh digunakan untuk membuat perbandingan kerana corak graf adalah hampir sama dan peratusan ralat di bawah 10 %. Kajian lanjut mengenai parameter yang mempengaruhi proses pembengkokan adalah penting pada masa akan datang.



## TABLE OF CONTENTS

		<b>Page</b>
<b>SUPERVISOR’S DECLARATION</b>		<b>ii</b>
<b>STUDENT’S DECLARATION</b>		<b>iii</b>
<b>ACKNOWLEDGEMENT</b>		<b>iv</b>
<b>ABSTRACT</b>		<b>v</b>
<b>ABSTRAK</b>		<b>vi</b>
<b>TABLE OF CONTENTS</b>		<b>vii</b>
<b>LIST OF TABLES</b>		<b>x</b>
<b>LIST OF FIGURES</b>		<b>xi</b>
<b>LIST OF SYMBOLS</b>		<b>xiii</b>
<b>LIST OF ABBREVIATIONS</b>		<b>xiv</b>
<b>CHAPTER 1</b>	<b>INTRODUCTION</b>	<b>1</b>
1.1	Introduction	1
1.2	Project Objective	2
1.3	Project Background	2
1.4	Problem Statement	2
1.5	Project Scope	2
	1.5.1 Flexure Bending	3
	1.5.1.1 Three Point Bending	4
	1.5.1.2 Four Point Bending	4
1.6	Research Flow	5
<b>CHAPTER 2</b>	<b>LITERATURE REVIEW</b>	<b>6</b>
2.1	Mild Steel	7
	2.1.1 Material Properties	7
2.2	Galvanized Steel	8
2.3	Bending Theory	11
2.4	Flexure Test	12
	2.4.1 Selection Of Flexure Tests	12
	2.4.2 Stress Distribution And Failure Nodes	14

2.5	Finite Element Method	16
	2.5.1 Finite Element Calculation	17
2.6	Theory of Bending Test	18
2.7	Finite Element Analysis Four Point Bending Test	22
	2.7.1 Stress Distribution with Linear Material Properties	22
	2.7.2 Stress Distribution with Nonlinear Material Properties	25
<b>CHAPTER 3</b>	<b>METHODOLOGY</b>	<b>26</b>
3.1	Introduction	26
3.2	Research Flow	27
3.3	Gather The Information	28
	3.3.1 Information from Internet	28
	3.3.2 Information Ump Thesis and Journal	29
	3.3.3 Information from Related Person	29
3.4	Design and Fabrication	30
	3.4.1 Test Rig Design	31
	3.4.2 Cutting Material	32
	3.4.3 Squaring Material	32
	3.4.4 Grinding	33
	3.4.5 CNC Software / Mastercam	34
	3.4.6 Tapering	34
	3.6.7 Turning	35
	3.6.4 Complete Test Rig	36
3.5	Four Point Bending Test	37
	3.5.1 Specimen Preparation	37
	3.5.1.2 Shearing Machine	37
	3.5.1.2 Strain Gauge	38
	3.5.2 Test Setup	39
	3.5.3 Test Procedure	41
3.6	Experiment And Simulation Flow Chart	43
3.7	Finite Element Model Four Point Bending	44
	3.7.1 The Material Properties	45
	3.7.2 Boundary Condition	45
	3.7.3 Process Step	45

<b>CHAPTER 4</b>	<b>RESULT AND DISCUSSION</b>	<b>46</b>
4.1	Introduction	46
4.2	Four Point Bending Test Result	46
4.3	Finite Element Simulation Result	52
	4.3.1 Simulation of Four Point Bending	52
	4.3.2 Result Simulation	54
4.4	Comparison of FE Simulation and Experimental	59
4.5	Discussion	61
<b>CHAPTER 5</b>	<b>CONCLUSION</b>	<b>64</b>
5.1	Introduction	64
5.2	Conclusion	64
5.3	Recommendations	65
<b>REFERENCES</b>		<b>66</b>
<b>APPENDICES</b>		<b>69</b>
A	Final Year Project 1 Gantt Chart	70
B	Final Year Project 2 Gantt Chart	71
C	Data From Experimental	72
D	Data From Simulation	73
E	Material Properties	74
F	Design Test Rig	74

**LIST OF TABLE**

<b>Table No.</b>	<b>Title</b>	<b>Page</b>
2.1	Coefficient of proposal equation for ultimate strain	7
2.2	Gain in $p_{max}$ and $e$ or possible weight reduction	20
2.3	Limits in $w/t$ for different section classes (sc)	20
2.4	Comparison of effective energy absorption for sections with different overall geometries and steel grades	22
2.5	Peak stresses for the four-point bending specimen	23
4.1	Result simulation	58
4.2	Comparison strain value experimental and finite element simulation	59

## LIST OF FIGURES

Figure No	Title	Page
1.1	Shimadzu machine	3
2.1	Comparison of reduction factors of elastic modulus predicted using the proposed equation with test results	8
2.2	Comparison of reduction factors of ultimate strength predicted using the proposed equation with test results	8
2.3	The fundamental concept in sheet metal bending	11
2.4	Three point bending setup	12
2.5	Four point bending setup	13
2.6	Four-point bending configurations	14
2.7	Moments and forces during the four-point bending	15
2.8	The finite element model used for the afpb test analysis	18
2.9	Maximum load pmax vs yield strength for bending tests	19
2.10	Four-point bending test geometry	23
2.11	The finite element model of four-point bending specimen (dimensions in mm)	23
2.12	Shear stress contours (mpa) in four-point bending specimen (linear material properties, roller diameter 20 mm).	24
2.13	Shear stress distribution in four-point bending specimen (linear material properties, 20-mm roller diameter)	24
2.14	Shear stress contours (mpa) in four-point bending specimen (nonlinear material properties, roller diameter 20 mm)	25
2.15	Shear stress distribution in four-point bending specimen (nonlinear material properties, 20-mm roller diameter)	25
3.1	General flow chart	28
3.2	Fabrication flow chart	30
3.3	Design test rig four point bending test	31
3.4	Bench saw cutting machine	32
3.5	Milling machine	33
3.6	Grinding machine	33
3.7	Mastercam software	34
3.8	Wire-cut EDM	35

3.9	Lathe machine	35
3.10	Design consideration in test rig fabrication	36
3.11	Shearing machine	37
3.12	Plates of galvanized steel (220mm x 33 mm x 1mm)	37
3.13	Bonded metallic strain gage	38
3.14	Four point bending test setup	39
3.15	Strain connected to data logger	39
3.16	Data logger connected to laptop	40
3.17	Strain gauge location on specimen during 4pbt	40
3.18	Specimen positioning inside the test rig during 4pbt	41
3.19	(a) The geometrical model for 4PBT (b) The meshed model for simulation	44
4.1	Condition specimen before bending process	47
4.2	The bended workpiece from inner span 100mm.	47
4.3	Graph times versus strain value for inner span 100mm	48
4.4	Graph times versus strain value for inner span 120mm	48
4.5	Graph times versus strain value for inner span 140mm	49
4.6	Condition specimen before bending process for free bend	50
4.7	Condition specimen after bending process	50
4.8	(A) Inner Span = 100mm, (B) Inner Span = 120mm, (C) Inner span 140mm, Result Experimental For Free Bending	51
4.9	Geometrical description of the simulation model	52
4.10	Striker start touching the workpiece	53
4.11	During bending process	53
4.12	After bending process	54
4.13	Result simulation for inner span 100mm	55
4.14	Result simulation for inner span 120mm	56
4.15	Result simulation for inner span 140mm	57
4.16	Graph comparison strain value experimental and FE simulation	59
4.17	Comparison length displacement after bend of experimental and FE simulation for inner span 100mm, 120mm And 140mm	60

## LIST OF SYMBOLS

$\sigma^2$	Variance
$P_{\max}$	Max bending load
$\mu$	Mean
$\eta$	Structural efficiency
$L$	Distance between load support
$R$	Normal anisotropic value
$\nu$	Poisson's ratio
$E$	Young's modulus
$t$	Sheet thickness
$\rho$	Neutral axis
$I$	Inertia moment of cross-section per unit width
$M(\alpha)$	Bending moment along the bending surface
$F_s$	Shear Force
$K$	Ultimate tensile strength
$t$	Sheet thickness
$\Delta K$	Spring back curvature
$M$	Bending moment
$R_e$	Yield Strength
$L$	Inertia moment of cross-section
$W$	Elastic Section Modulus
$h$	Specimen width

**LIST OF ABBREVIATIONS**

AISI	American Iron and Steel Institute
ASTM	American Society for Testing and Material
TRIP	Transformation Induced Plasticity
CNC	Computer Numerical Control
UTS	Ultimate Tensile Strength
SHS	Square Hollow Sections
EHS	Element Hollow Sections
FEA	Finite Element Analysis
LVDT	Linear Variable Displacement Transducers
PDE	Partial Differential Equations
FEM	Finite Element Method
CHS	Circular Hollow Sections
RHS	Rectangular Hollow Sections
CAD	Computer-Aided Design
EDM	Electric Discharge Machining
3PBT	Three Point Bend Test
4PBT	Four Point Bend Test
DAQ	Data Acquisition System
AFPB	Asymmetric four-point bending tests



## **CHAPTER 1**

### **INTRODUCTION**

#### **1.1 INTRODUCTION**

Four-point bending has several advantages. Firstly, it produces a uniform moment between the two inner loading rollers in the specimen which gives rise to a uniform maximum tensile stress in the specimen surface. Secondly, no special sample gripping is needed for the four-point bend test, which makes it possible to test brittle materials in tension and makes sample preparation relatively simple since a specimen with a uniform rectangular cross-section is usually used in the test. Thirdly, sample mounting and dismounting are fairly straightforward in four-point bend, which is particularly convenient for high temperature tests in which sample mounting and dismounting can be a non-trivial matter in bending test. Furthermore, using four-point bend a pure shear stress can be applied to a test piece by asymmetrically loading the specimen. Because of these advantages four-point bending can be a convenient test method for bending studies, especially for studying on the effect of inner span since the specimen for four-point bend has a flat surface on which a uniform tensile stress is applied. The effect of inner span at different stages for surface microscopic examination can also be fairly straightforward because of easy sample mounting and dismounting.

## **1.2 PROJECT OBJECTIVE**

Fabrication and performing the four point bending test on the selected mild steel.

The objectives of this research are;

1. Design & fabricate test rig for four point test
2. Establish experiment concentrates on the effect of inner span in four-point bending test.
3. Comparison analysis FEA simulation on four point bending test

## **1.3 PROJECT BACKGROUND**

Steel one of the important materials used in the construction of roads, railways, other infrastructure, appliances, and buildings. Steel is used in a variety of other construction materials, such as bolts, nails, and screws. In this project, the effect of inner span in four- point bending test will be studied. The mild steel work piece will be prepared. The effect of inner span on mild steels work piece on flexural strength, the 4 four point bending test will be conducted. The experiment will be conducted of all input parameters using finite element application.

## **1.4 PROBLEM STATEMENT**

For problem statement for this research is to emphasize on inner span setting.

## **1.5 PROJECT SCOPE**

This focus is based on the following aspect:

- a) To design and fabrication fixtures for four point bending test on Shimadzu Machine as figure1.
- b) The tested material is mild steel.
- c) Experiment will conducted to validate of all input parameters.

- d) Make simulation using the finite element software like Abaqus, Algor or patran.
- e) The effect of the known parameters will be tested
- f) Similar test condition will be used to compare the result



**Figure 1.1:** Shimadzu machine

### **1.5.1 Flexure Bending**

A flexure/bending test, also known as a bend test, is used to determine the strength of a material by applying force to the item in question and seeing how it reacts under pressure. Typically the bend test measures ductility, the ability of a material to change form under pressure and keep that form permanently. In certain cases the bending test can determine tensile strength. When using the bend test for this purpose, testers examine which side of the material breaks first to see what type of strength the material has. It also lets them know what kinds of pressure it holds up against and what kinds it doesn't.

Ductility describes how well a material, usually metal, can be stretched and keeps its new shape. Steel, for example, is highly ductile. If pressure is applied that stretches the steel into a new shape, it will keep this shape even after the pressure has been removed.

To determine how ductile a material is, a bending test is used. Force is applied to a piece of the material at a specific angle and for a specific amount of time. The material is then bent to a certain diameter using force. After the bending test is over, the material is examined to see how well it held its shape once the pressure was removed, and whether or not the material cracked when pressure was applied. Bending tests are used for determining mechanical properties of unidirectional composite materials. Due to the important influence of shear effects in the displacements, great span-to-depth ratios are used in order to eliminate these effects.

#### **1.5.1.1 Three bending**

Three-point short-beam bending used for measuring the interlinear shear strength of metal because of the simplicity of the test

#### **1.5.1.2 Four-point bending**

Four-point test configurations are used in order to obtain flexural strength and flexural modulus. The rotation of the cross sections in the deformation process leads to the contact zone between specimen and cylindrical supports changing in a three-point bending test. Furthermore, in a four-point bending test the contact between specimen and cylindrical loading noses also changes.

## 1.6 RESEARCH FLOW

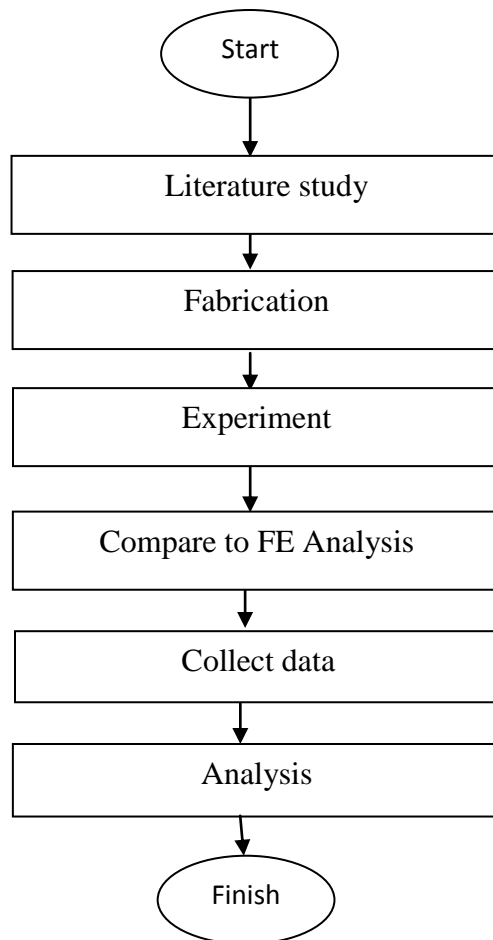


**Figure 1.2:** Research flow chart

## **CHAPTER 2**

### **LITERATURE REVIEW**

#### **2.1 MILD STEEL**

Mild steel is a type of steel alloy that contains a high amount of carbon as a major constituent. An alloy is a mixture of metals and non-metals, designed to have specific properties. Alloys make it possible to compensate for the shortcomings of a pure metal by adding other elements. To get what mild steel is, one must know what the alloys that are combined to make steel are. So, let us see what we mean by steel, which will help us in understanding what mild steel is and also in understanding the properties.

Steel is any alloy of iron, consisting of 0.2% to 2.1% of carbon, as a hardening agent. Besides carbon, there are many metal elements that are a part of steel alloys. The elements other than iron and carbon, used in steel are chromium, manganese, tungsten and vanadium. All these elements along with carbon, act as hardening agents. That is, they prevent dislocations from occurring inside the iron crystals and prevent the lattice layers from sliding past each other. This is what makes steel harder than iron. Varying the amounts of these hardening agents creates different grades of steel. The ductility, hardness and mild steel tensile strength are a function of the amount of carbon and other hardening agents, present in the alloy. The amount of carbon is a deciding factor, which decides hardness of the steel alloy. A steel alloy with a high carbon content is mild steel, which is

in fact, much harder and stronger than iron. Though, increased carbon content increases the hardness of the steel alloy.

Mild steel can also be described as steel which is not stainless steel. Mild steel differs from stainless steel in its chromium content. Stainless steel contains a lot more chromium than ordinary carbon or mild steel.

### 2.1.1 Material Properties

A series of tensile coupon material tests at elevated temperatures on quenched and tempered high strength steel BISALLOY80 and mild steel XLERPLATE Grade 350 using both steady and transient state test methods has been performed by [Chen et al]. In this study, a unified equation to determine the yield strength (0.2% proof stress), elastic modulus, ultimate strength and ultimate strain of high strength steel and mild steel for temperatures ranged from approximately 22 to 1000 has been proposed, The values of coefficients  $a$ ,  $b$ ,  $c$  and  $n$  of the equations are calibrated with the high strength steel and mild steel test results, and the coefficients are presented in Tables 2.1. Graph reduction factors of elastic modulus and ultimate strength show in figure 2.1 and 2.2

**Table 2.1:** Coefficient of proposal equation for ultimate strain

	Temperature (°C)	$22 \leq T < 540$	$540 \leq T \leq 1000$	
High strength steel	$a$	1.0	0.25	
	$b$	22	540	
	$c$	$3.58 \times 10^5$	215	
	$n$	2	0.5	
	Temperature (°C)	$22 \leq T < 150$	$150 \leq T < 720$	$720 \leq T \leq 1000$
Mild steel	$a$	1.0	0.677	0.1
	$b$	22	150	720
	$c$	35	$3.22 \times 10^8$	420
	$n$	0.5	3	0.5

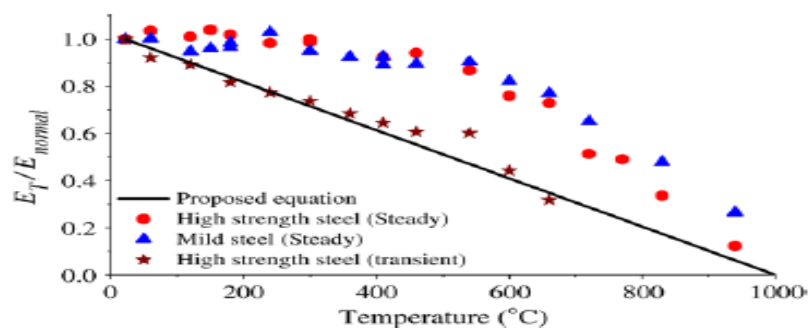


**Figure 2.1:** Comparison of reduction factors of elastic modulus predicted using the proposed equation with test results.

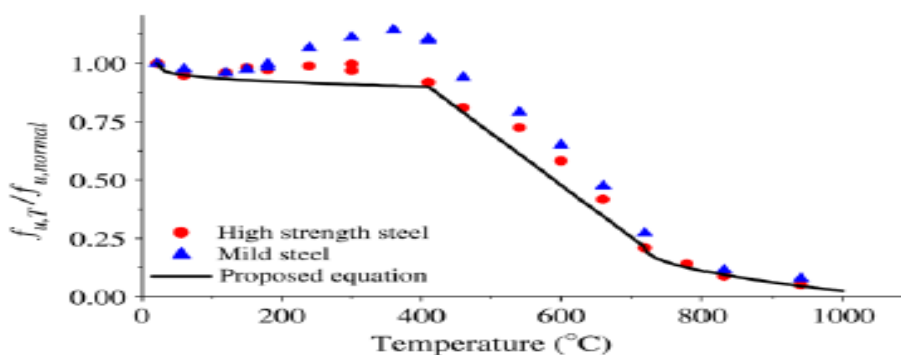


**Figure 2.2:** Comparison of reduction factors of ultimate strength predicted using the proposed equation with test results.

## 2.2 GALVANIZED STEEL

Hot-dip-zinc-coated steel sheet, also called galvanized sheet, is by far the most widely used coated sheet product. For general applications, the galvanized sheets have 19  $\mu\text{m}$  of zinc thickness per side. This corresponds to a two-side coating mass of 275 g/m. Heavier coatings are used in applications which require higher corrosion resistance, such as highway drainage culverts. In the automobile industry, where formability and weldability are key considerations, lighter coatings such as 90 g/m<sup>2</sup> are more typical (Townsend, 1993). The galling, a form of adhesive wear, affects the cost of forming steel in automotive stamping since it increases die maintenance costs and scrap rates (Kim et al., 2008).



Most of the coating is nearly pure zinc. There is an intermetallic layer containing about 6 % Fe, between the substrate and the zinc coating. Aluminium, typically in the range of 0.1 % to 0.2 %, is added to the zinc bath in order to prevent the formation of a thick, continuous zinc-iron intermetallic layer that could lead to poor coating adhesion during forming. Aluminium reacts preferentially with the steel to form a thin iron-aluminium intermetallic layer which acts as a barrier and delays the growth of the zinc-iron intermetallic layer.

Galvalume® is the trade name of steel sheets coated with 55%Al-Zn alloy. It is applied by a continuous hot dip process similar to that of galvanized coatings. This coating combines the durability of aluminium and the galvanic protection of the zinc, resulting in a product which shows excellent corrosion resistance in marine and industrial environments, high temperature oxidation resistance, heat reflectivity of the aluminium coatings and a pleasant and distinctive appearance.

The chemical composition of the coating is 55 % of Al, 43.5 % of Zn and 1.5 % of Si and it is composed of a three-phase structure as described below (BHP Steel, 1994a):

- a) A thin quaternary alloy layer, composed of Al, Zn, Fe and Si, between the steel base and the main coating layer;
- b) An aluminium rich dendritic phase (80 % by volume) and
- c) A zinc rich interdendritic phase.

All the three phases are necessary to provide the improved corrosion resistance properties. The zinc-rich phase gives the coating its galvanic protection ability, a similar property to a normal galvanized coating. The aluminium rich phase and the alloy layer provide to the coating its durability once the zinc-rich phase is consumed. About 1.5 % silicon is added to the molten bath in order to control the growth of the alloy layer during the dipping process (BHP Steel, 1994a).

As the specific weight of aluminium is lower than that of the zinc, the 55%Al-Zn coating is lighter than the zinc coating, both with same coating thickness. For instance, the weight of the zinc coating designed as G90 (ASTM A653) is  $275 \text{ g/m}^2$  while the weight of 55%Al-Zn coating designed as AZM150 (ASTM A792) is  $150 \text{ g/m}^2$ . Notice that both coatings have about the same thickness of  $20 \text{ }\mu\text{m}$  per side which results in higher covering area per ton of Galvalume® compared to a galvanized product. As an example of the difference, one ton of 0.45 mm Galvalume® can cover 4.5 % more area than the same thickness of a galvanized sheet (BHP Steel,1994b).

The 55%Al-Zn coating shows long-term atmospheric corrosion resistance due to the combination of the durability of aluminium which acts as a mechanical barrier and the galvanic protection given by zinc (Gronostajski, 1995). Exposition tests of the zinc coated steel sheet (coating G90) and Galvalume® (coating AZM 150) were done by Bethlehem Steel. The test panels were exposed at rural, industrial, moderate marine and severe marine environments.

The results showed that the corrosion resistance of the 55%Al-Zn is generally at least two to four times higher than that of an equal thickness of galvanized coating (BHP Steel, 1994a). Recent work found that the zinc coating experiences a degree of corrosion between 1.7 times (marine-industrial atmosphere) and 4.5 times (rural atmosphere) greater than that of the 55%Al-Zn coating, considering the results obtained after five years of atmospheric exposure (Palma et al., 1998).

The steel sheet coated with 55%Al-Zn alloy can be used at higher temperature conditions compared to the zinc coated steel sheet. In terms of appearance at higher temperatures, Galvalume® maintains its superficial brightness up to  $320 \text{ }^\circ\text{C}$ , while the galvanized sheet maintains its brightness up to  $230 \text{ }^\circ\text{C}$  (BHP Steel, 1994c).

### 2.3 BENDING THEORY

In this section a brief review of fundamentals in sheet metal bending are discussed. The main point is to explain how the process occurs in term of the mechanics of sheet metal bending. The existence of internal stress distribution along the part thickness is illustrated in Figure 2.3. In this example, the used material is assumed as elastic, perfectly-plastic with no strain hardening. Other than that, bending occurs under plane strain conditions and the neutral axis is located at the middle of sheet metal cross-section.

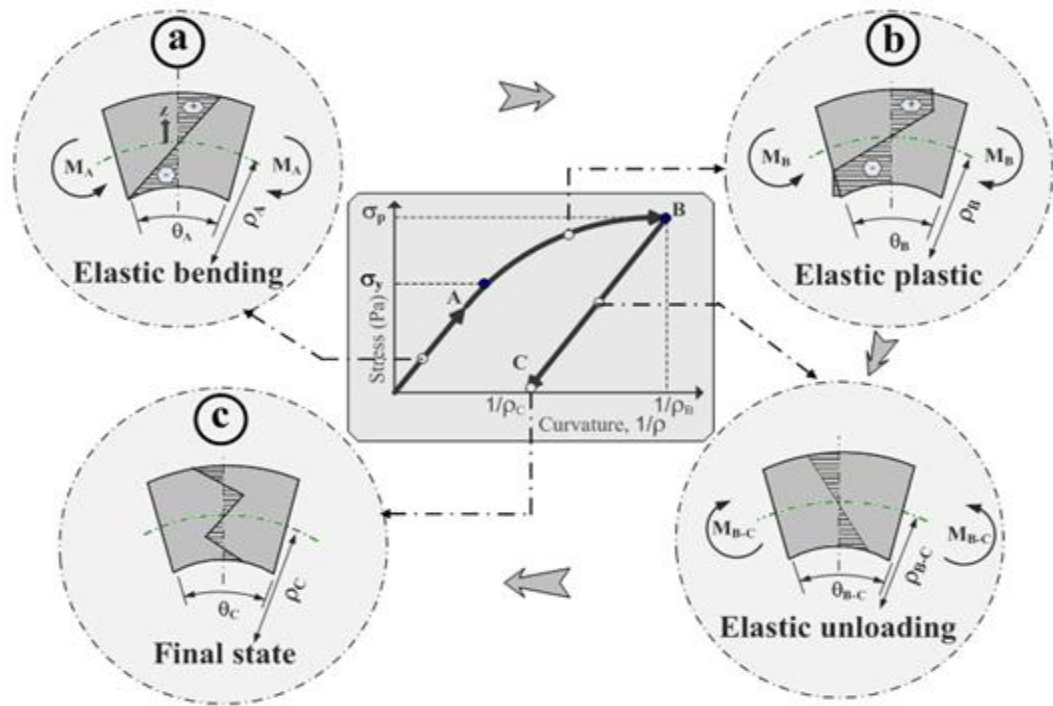


**Figure 2.3:** The fundamental concept in sheet metal bending

## 2.4 THE FLEXURE TEST

This topic a brief review about the fundamental of the flexure test is discussed. The flexure test method measures behavior of materials subjected to simple beam loading. It also known as transverse test, three point bending test, four point bending test. Flexural tests to determine the mechanical properties of resins and laminated fibre composite materials is widespread throughout industry owing to the relative simplicity of the test method, instrumentation and equipment required. Using this method, the workpiece is placed on a support span and the load is applied in between of the support at a specified rate. During the test, the workpiece is subjected to compressive stress at the concave surface and tensile stress at the convex surface. Flexure testing is often done on relatively flexible materials like polymers, wood and composites. It is obvious that this test is mostly applied for the flexible materials where the material properties cannot easily obtained from the tensile tests. Among the most parameters are the flexural strength, the flexural modulus and the modulus of rupture.

### 2.4.1 Selection of the Flexure Tests

This subsection discuss about why the flexure test method are choose for this research. There are two method most usually used for the determination of the flexural properties of laminates. There are three point bend test (3PBT) and four point bend test (4PBT) that illustrated schematically in figure 2.4 and 2.5. For this research, 4PBT has been chosen as a method test.

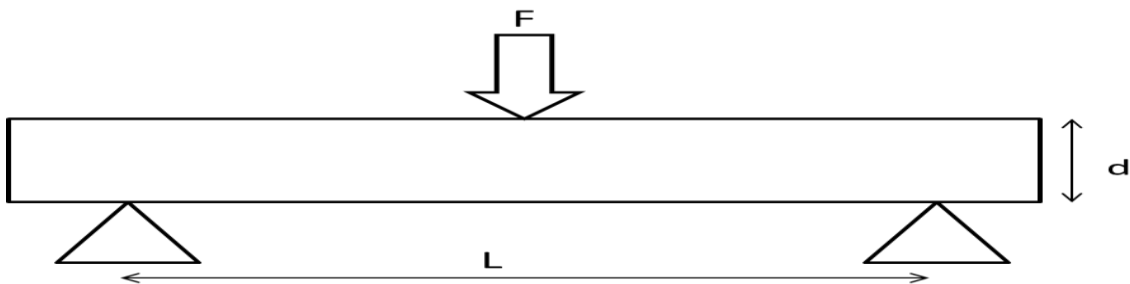


**Figure 2.4:** Three point bending setup

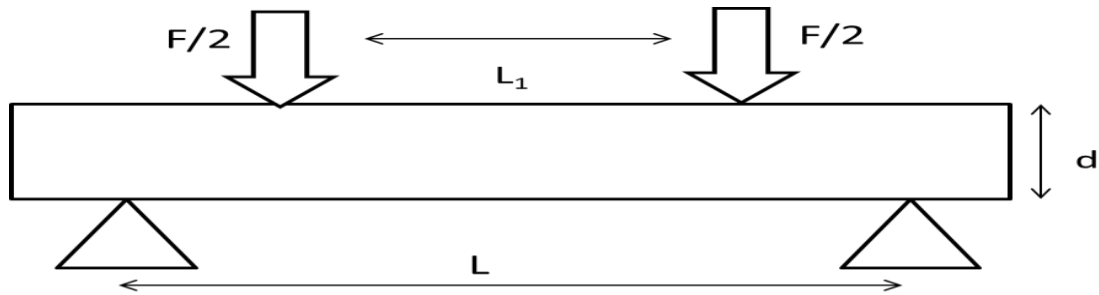


**Figure 2.5:** Four point bending setup

For 3PBT, the workpiece is supported on two outer points, and deformed by driving the third central point downwards. It has a major advantage which involves the shortest possible effective gauge length of any testing method. This is because the maximum stress in three point bending falls off linearly with distance from the center.

The 4PBT has two adjacent loading rollers as a driving force. It is moved downward typically at similar and constant speed against the sample supported by the outer support. The major advantage of 4PBT is it creates a constant moment stress between the inner span. It is suitably used to determine part strength for design purposes where the center span is uni-axially stressed and no shear stresses exist.

#### **2.4.2 Stress Distribution and Failure Modes**

It is essential to understand stress distribution and failure modes in 4PBT. Stress distributions depend on geometry of test piece and the length between rollers as shown in Figure 2.6.

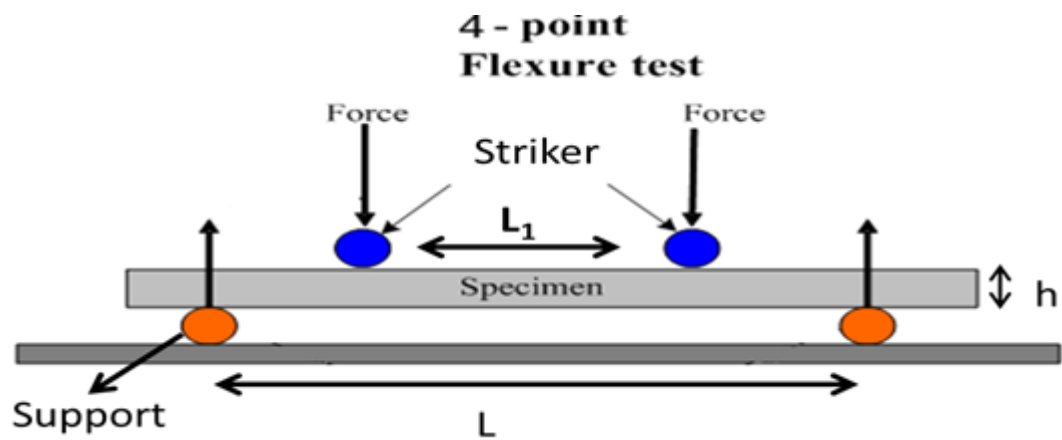
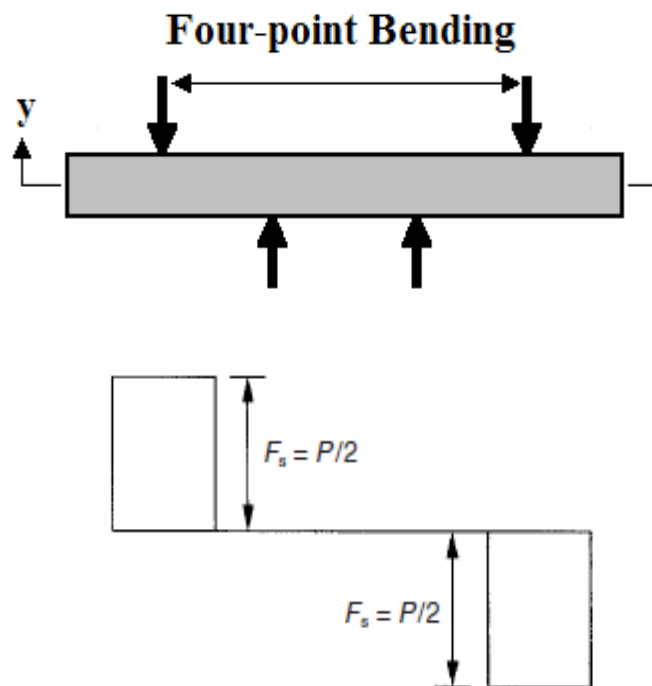


**Figure 2.6:** The four-point bending configurations

In a four-point bending test, a constant moment is developed between inner span as shown in Figure 2.7.



a) Shear force diagram

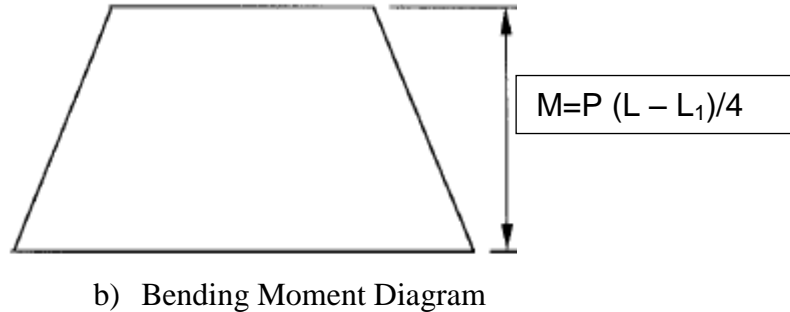


**Figure 2.7:** Moments and forces during the four-point bending

Clearly stress concentrations exist at the loading points but in four-point loading, between the inner loading points, there is a constant bending moment. Figure 4.6 shows the variation in normal stress, caused by bending moment, and shear stress, caused by shear force, assuming a rectangular specimen cross-section.

In Figure 4.5 to 4.6 the material properties are assumed to be uniform through the thickness because they are in unidirectional composites or isotropic materials. Under these circumstances the normal stress varies linearly from a maximum in compression on one surface to an equal maximum in tension on the other surface, passing through zero at the mid-plane, which is usually called the neutral axis. The maximum normal stress is given by Equation [2.1]:

$$\sigma = \frac{6M}{bh^2} \quad (2.1)$$

where  $M$  is the bending moment,  $b$  and  $h$  being the specimen width and thickness, respectively. The distribution of shear stress is parabolic, with a maximum at the neutral axis and zero at the outer surfaces of the beam; the maximum value is given by Equation [2.2]

$$\tau = \frac{3F_s}{2bh} \quad (2.2)$$

where  $F_s$  is the shear force on the specimen cross-section.

The flexural response of the beam is obtained by recording the load applied and the resulting strain. The strain can be measured by bonding strain gauge to the tensile surface of the beam, or by measuring the displacement at the center of the beam and assuming that beam theory applies, so that strains can be calculated. The bending moment,  $M$ , is a function of the measured load and specimen geometry, so that the applied stress can be calculated from Equation [2.1] and the full stress–strain behavior of the beam in bending can be obtain.

In four-point bending the bending moments increase linearly from zero at the supports to a maximum at the loading points and are constant between these points, as shown in Fig. 2.7. The shear force and inter laminar shear stress are zeroed between the loading points, so that this central portion of the beam is subjected to a pure bending moment.

## **2.5 FINITE ELEMENT METHOD**

The finite element method (FEM) (its practical application often known as finite element analysis (FEA)) is a numerical technique for finding approximate solutions of partial differential equations (PDE) as well as integral equations. The solution approach is based either on eliminating the differential equation completely (steady state problems), or rendering the PDE into an approximating system of ordinary differential equations, which are then numerically integrated using standard techniques such as Euler's method, Runge-Kutta.

In solving partial differential equations, the primary challenge is to create an equation that approximates the equation to be studied, but is numerically stable, meaning that errors in the input and intermediate calculations do not accumulate and cause the resulting output to be meaningless. There are many ways of doing this, all with advantages and disadvantages. The finite element method is a good choice for solving partial differential equations over complicated domains (like cars and oil pipelines), when the

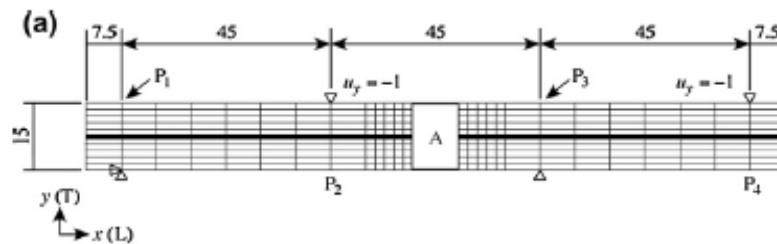


domain changes (as during a solid state reaction with a moving boundary), when the desired precision varies over the entire domain, or when the solution lacks smoothness. For instance, in a frontal crash simulation it is possible to increase prediction accuracy in "important" areas like the front of the car and reduce it in its rear (thus reducing cost of the simulation). Another example would be in Numerical weather prediction, where it is more important to have accurate predictions over developing highly-nonlinear phenomena (such as tropical cyclones in the atmosphere, or eddies in the ocean) rather than relatively calm areas.

### 2.3.1 Finite Element Calculations

To determine the crack geometry factor  $f(2a/s)$ , three-dimensional FEM calculations (Cicilia., et al) were performed using ANSYS version 5.7 from the Information Initiative Center of Hokkaido University. Fig. 2.8 shows the finite element mesh of the AFPB specimen.

The crack length  $2a$  varied from 1 to 8 mm at intervals of 1 mm. The mesh was refined closer to the crack tip, as shown in Fig. 2.8c and d. The length, thickness, and width directions of the model were defined as the x-, y-, and z-directions, respectively. These directions corresponded to the longitudinal (L), tangential (T), and radial (R) directions of the wood. A crack was produced along the L direction in the LT plane, which is the so-called TL system.



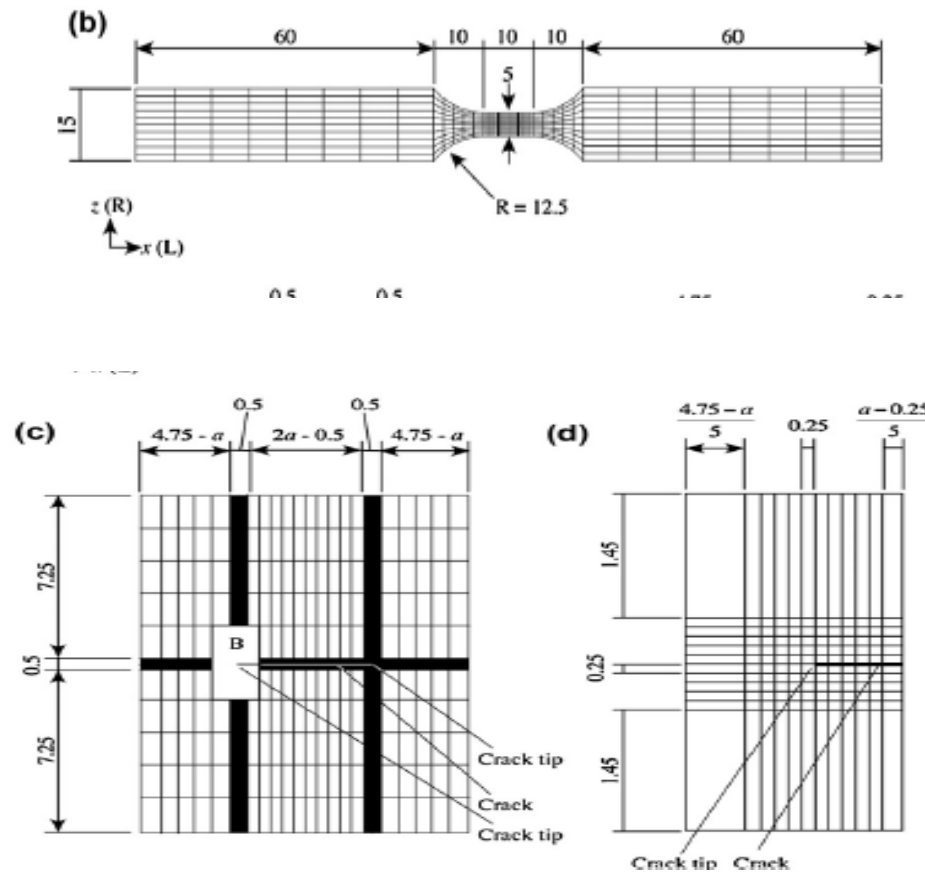


**Figure 2.8:** The finite element model used for the AFPB test analysis. Unit= mm L.T and represent the longitudinal, tangential and radial directions. (a) Top view of the overall mesh,(b) side view of the overall mesh, (c) detail of zone A in (a) and (d) detail of Zone B in(c).

## 2.6 THEORY OF BENDING TESTS

Bending tests related to the application of high strength steels for example in door intrusion beams have been performed on rectangular tubes 50x30xt mm by (Jan Olof Sperle.et al). The thickness t has varied from 1 to 2 mm. A few tests have also been performed with square tubes with dimensions 30x30x2, 25x25x2 mm and some on circular tubes. Cold-rolled dual-phase and micro alloyed steels as well as two hot-rolled micro alloyed steel have been included. Some tubes were manufactured in shop by roll forming and continuous resistance welding. All other test specimens were manufactured in

laboratory by bending and manual arc welding. The bending tests were carried out in three-point bending. The distance between the supports was, with a few exceptions,  $L = 800$  mm. During the test the load displacement plot was recorded. The maximum deformation was 150 mm. For further analysis  $P_1$ , load at 1 mm plastic deformation and  $P_{max}$ , the ultimate load as well as the absorbed energy was evaluated. As expected the load-bearing capacity increases with increasing yield strength. Results expressed as ultimate load  $P_{max}$  are plotted against yield strength in Figure 2.9.

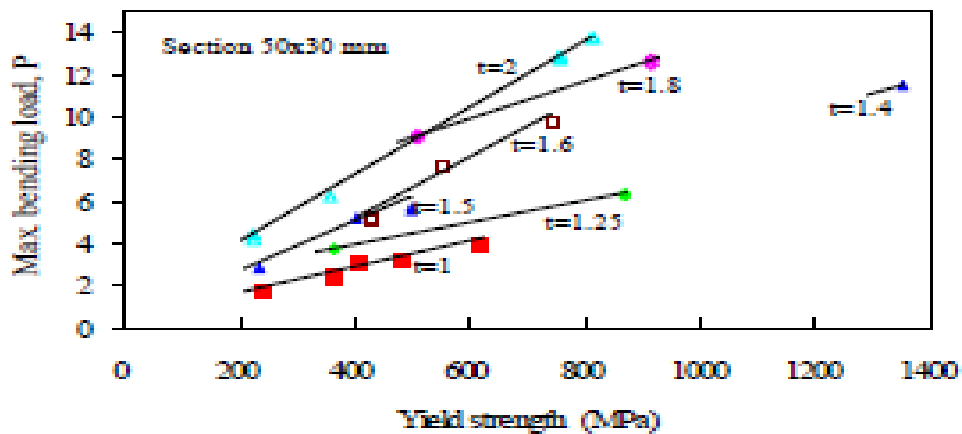


**Figure 2.9:** Maximum load  $P_{max}$  vs yield strength for bending tests

Similar relations as shown in Figure 2.9 are obtained if  $P_1$  and the energy absorption  $E$  are plotted against the yield strength. For the purpose of generalization a multiple regression analysis have been performed on the results for sections 50 x 30 mm. This gives:

$$P_1 = 0.00771 Re^{0.933} t^{1.629} \text{ (kN)} \quad (3.1)$$

$$P_{max} = 0.01804 Re^{0.839} t^{1.426} \text{ (kN)} \quad (3.2)$$

$$E = 7.1304 Re^{0.571} t^{1.882} \text{ (J)} \quad (3.3)$$

Using the above results from the regression analysis we can draw some practical conclusions as to possible weight reductions or increases in maximum load  $P_{max}$  when using high strength steel sheet instead of mild steel in door impact beams, Table 2.2.

**Table 2.2:** Gain in Pmax and E or possible weight reduction

Grade	Gain with unchanged thickness, %		Weight reduction %	
	P <sub>max</sub>	E	P <sub>max</sub>	E
Docol 600	79	49	33	19
Docol 800	123	73	43	25
Docol 1000	179	101	51	31
Docol 1200	233	127	57	35
Docol 1400	286	151	61	39

Based on yield strength, thickness, overall design, and loading conditions a theoretical load Pmax can be predicted for all specimens tested by using a method described in the Steel Sheet Handbook (4). The model takes buckling into account by using an effective thickness concept. Cross sections which buckles before the nominal stress in the flanges reaches the yield stress are categorized in cross section class 3. Cross sections that can be bent plastically without buckling are categorized in SC = 1 and cross sections in between those limits in SC = 2.

The structural efficiency  $\eta$  of a bent cross section is related to section class, SC. This as well as the limiting value in width to thickness ratios, w/t, between section classes is shown in table 2.3 for rectangular sections in steel

**Table 2.3:** Limits in w/t for different section classes (SC)

Yield strength R <sub>s</sub> (MPa)	SC 1	(w/t) <sub>1-2</sub> = 454 $\sqrt{1/R_s}$	SC 2	(w/t) <sub>2-3</sub> = 518 $\sqrt{1/R_s}$	SC 3
200	$\eta > 1$	32	$\eta \approx 1$	37	$\eta < 1$
400		23		26	
600		19		21	
800		16		18	
1000		14		16	
1200		13		15	
1499		12		14	

The load bearing capacity,  $P_{max}$ , for a bent tube is given by:

$$P_{max} = \frac{4 \cdot R_e \cdot W \cdot \eta}{L} \quad (3.4)$$

where  $R_e$  = yield strength

$W$  = elastic section modulus

$\eta$  = structural efficiency

$L$  = distance between load supports

Besides by using the Steel Sheet Handbook (4) the following analytical expression for the structural efficiency can be used to calculate.

$$\eta = 1.122 [0.7 + 0.52 \exp \{-5 \cdot 10^{-6} (w/t \sqrt{R_e - 200})^{1.93}\}] \quad (3.5)$$

where  $\eta$  = structural efficiency

$w$  = width of compression flange

$t$  = thickness of compressed flange

$R_e$  = yield strength (MPa)

Maximum loads predicted with the above described method are in good agreement with the experimental values. The regression coefficient is  $r^2 = 0,98$  and the standard deviation in  $P_{max}$  is + 0,53 kN.

The absorbed energy when bending the tubes is also related to the structural efficiency of the beam. If buckling takes place before the nominal maximum stress reaches yield stress, i.e.  $\eta < 1$ , the load-deflection curve decreases rather quick after the maximum load  $P_{max}$  has been reached and the efficiency in energy absorption will decrease.

This can be exemplified by studying results from beams with different cross sections and steel strength levels. In the table 2.4 different cross sections are compared in terms of efficiency in absorbed energy.

**Table 2.4:** Comparison of effective energy absorption for sections with different overall geometries and steel grades

Cross section mm	Grade	w/t (r/t)	(w/t) <sub>1-2</sub> (r/t) <sub>1-2</sub>	SC	$\eta$	E J	G kg/m	E/G J/kg/m	Relation
50x30x2	Docol 350 YP $R_m =$ 350-400	23	23	1	1.16	718	2.40	299	1 ref
30x30x2		10	23	1	1.20	693	1.76	393	1.31
25x25x2		10	23	1	1.22	540	1.45	372	1.24
$\varnothing$ 27x2	Docol 1000 $R_m =$ 800-900	6.8	18	1	1.37	364	1.23	295	0.99
$\varnothing$ 32x2		7.5	18	1	1.35	453	1.48	306	1.02
50x30x2		23	15	3	0.96	1213	2.40	505	1.69
30x30x2	13	15	1	1.20	1239	1.76	704	2.35	
25x25x2	10	15	1	1.22	1053	1.45	726	2.43	

From Table 2.4 we can observe that changing steel from Docol 350 YP to Docol 1000 for the 50x30x2 mm section increases the specific energy absorption E/G by 69 %. Reducing the flange width by using a section 30x30x2 mm in grade Docol 1000 gives a further increase in specific energy absorption to totally 135 % compared to the 50x30x2 mm section in grade Docol 350 YP. Reducing the flange width reduces w/t and improves the section class from SC = 3 to SC = 1. If we compare circular tubes with the rectangular ones, the circular tubes show lower specific energy although the cross section is fully effective (SC = 1). This is because the nominal section modules to weight ratio (W/G) is less for circular than for rectangular tubes

## 2.7 FINITE ELEMENT ANALYSIS FOUR BENDING TEST

### 2.7.1 Stress Distribution with Linear Material Properties

The specimen geometry for the four-point beam test is shown in Fig. 2.10. Only half of the specimen needs to be modeled as a result of symmetry. The finite element model of the four-point bending specimen is shown in Fig. 2.11. The specimen modeled is 32 plies thick. The nominal value of the thickness of 4-062 mm is used (Fig. 2.11). (Wei Cheng. Et al) choose  $T_1 = T_3 = 0.254\text{mm}$ , with five elements in each region.  $T_2 = 3.554\text{ mm}$  with 10 elements in this region. The total length of the specimen is 50 mm. The span is 40 mm. The distance between the two loading rollers is 20 mm.

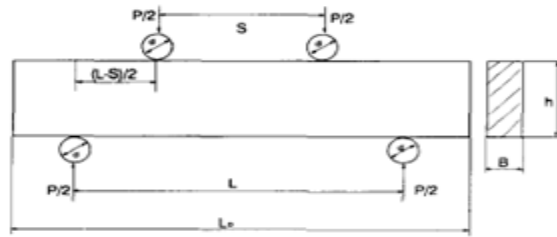


**Figure 2.10:** Four-point bending test geometry

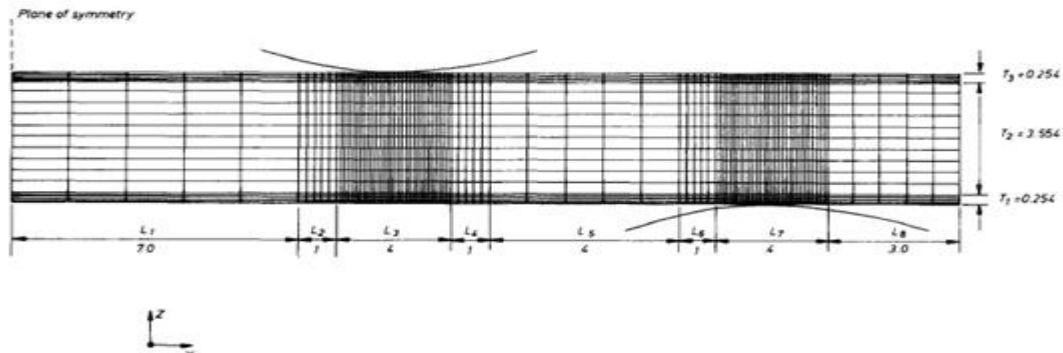


**Figure 2.11 :** The finite element model of four-point bending specimen (dimensions mm)

Other details of the finite element analysis are the same as before. The peak stresses are listed in Table 2.5.

**Table 2.5:** Peak stresses for the four-point bending specimen

Case	$\sigma_x^{\max}$ (MPa)	$\sigma_x^{\min}$ (MPa)	$\sigma_z^{\min}$ (MPa)	$\tau_{xz}^{\max}$ (MPa)
Linear	688	-1 149	-330	101
Nonlinear	788	-1 207	-315	78
Difference (%)	15	5	-5	-23

The shear stress contours for the four-point bending specimen are shown in Fig. 2.12 and the shear stress distributions at various sections are compared with beam theory in Fig. 2.13. It should be noted that section B is the one at which the maximum shear stress occurs. The shear stress here is marginally higher than close to the support rollers. From

these figures it can be seen that, as before, a high stress concentration occur in the very small region in the vicinity of the loading and supporting rollers. The parabolic assumption is very good for the sections between C and E. However, for sections between A and C and between E and G, this assumption is not valid. It is found that the maximum shear stress does not occur in the middle of the section; instead, it occurs near the top surface close to the loading roller. The maximum value of shear stress is also higher than that from beam theory but only by a factor of 1-14.

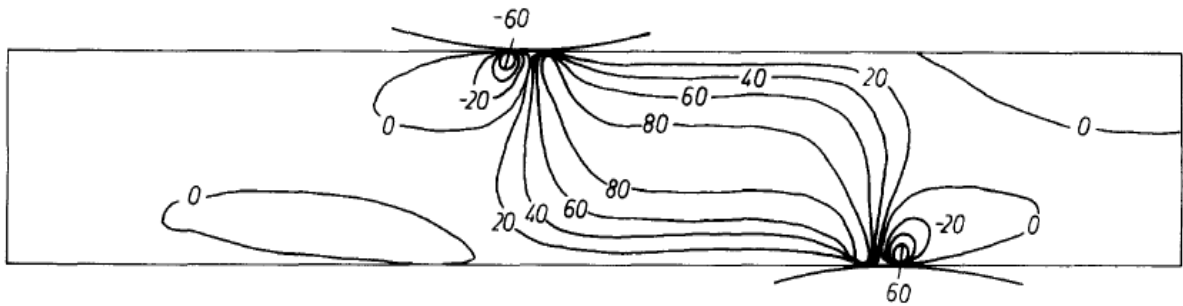


**Figure 2.12:** Shear stress contours (MPa) in four-point bending specimen (linear material properties, roller diameter 20 mm).

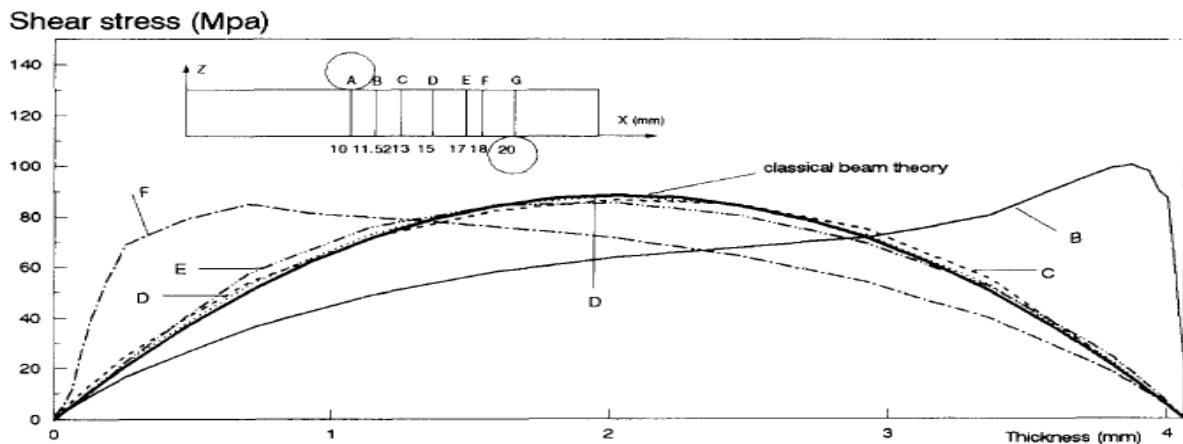


**Figure 2.13:** Shear stress distribution in four-point bending specimen (linear material properties, 20-mm roller diameter)



### 2.5.2 Stress distribution with nonlinear material properties

Nonlinear analysis of the four-point bending specimen has also been carried out. The material properties are the same as for the three-point bending case. The finite element mesh and other details are the same as for the linear material case. It can be seen that the influence of nonlinearity on the maximum shear stress is significant. Therefore, this influence should be taken into account in the stress analysis. The shear stress contours for the four-point bending specimen are shown in Fig. 2.14. The shear stress distributions at various sections are compared with beam theory in Fig. 2.15.

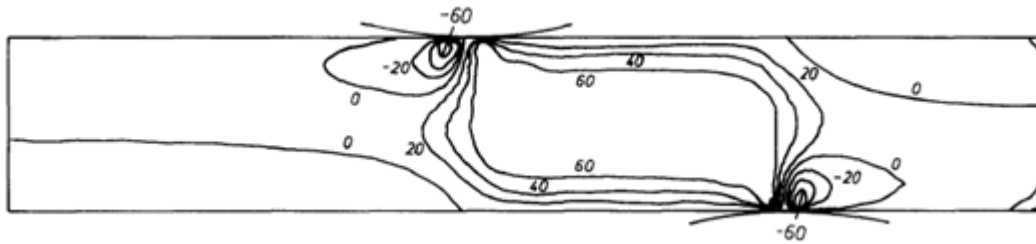


**Figure 2.14:** Shear stress contours (MPa) in four-point bending specimen (nonlinear material properties, roller diameter 20 mm).

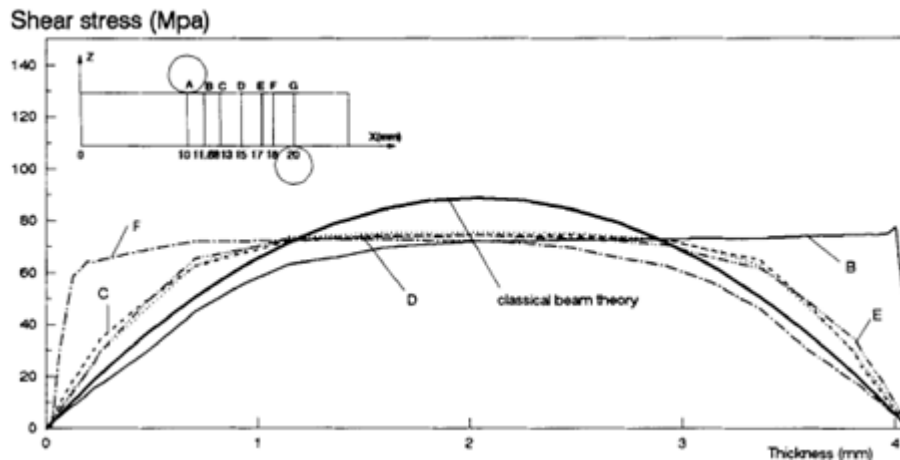


**Figure 2.15:** Shear stress distribution in four-point bending specimen (nonlinear material properties, 20-mm roller diameter)

## **CHAPTER 3**

### **METHODOLOGY**

#### **3.1. INTRODUCTION**

This project was mainly about design and fabrication four-point bending test rig for experimental on the effect of various inner span setting on part performance. In general, this project mainly used the four point bending test method as other researchers. With different apparatus and approach, the experiment was conducted in order to get the result and achieve the objective. This is important since other researchers already proved that the model and apparatus used were capable to give the desired result.

Methodology is essential step to be made and consideration before in order to complete any project or experiment. The main reason to do methodology is to assure that the project will be made just in time and work smoothly until it is finished as well as planning. With fine methodology, it will ensure the project or experimental follow the guideline based on the objectives. The most important part in methodology is to plan the step or the structure to conduct experiment related to objective of this project. Besides that, this methodology also make easier to indicate the problem in our project because it has step by procedure. It also will help this project move smoother and faster with this structure methodology.

Referring the Gantt chart shown in the appendix, this final year project (FYP) get started with some introduction or briefing by supervisor. In beginning of several first weeks management schedule has been setup for this project which covered the whole week in the future. Then, this project was continuing with literature review, find and gather all the information from internet, journal, reference book and related person related to this project. After that, make a design one fixture, sticker and coupling for four-point bending test rig experiment tool. Then, this project continues by fabricate a new test rig as well as the design. Then, make an experiment four point banding test and come out with data collection. The result will compare by make a simulate using finite element method software. The data will make an analysis to the final result and conclude.

Lastly, the final report writing and prepare the final preparation. This process will be predicted to be finished in one week to arrange and accomplish. A report is guided by UMP thesis format and also guidance from supervisor. All task scheduled is taking around fourteen weeks to complete.

### **3.2. RESEACRH FLOW**

To achieve the objectives of the project, a methodology were construct base on the scope of product as a guiding principal to formulate this project successfully. The terminology of the work and planning can be seen in the flow chart below. The flow chart is very important in methodology to make sure that the experiment in the right direction.

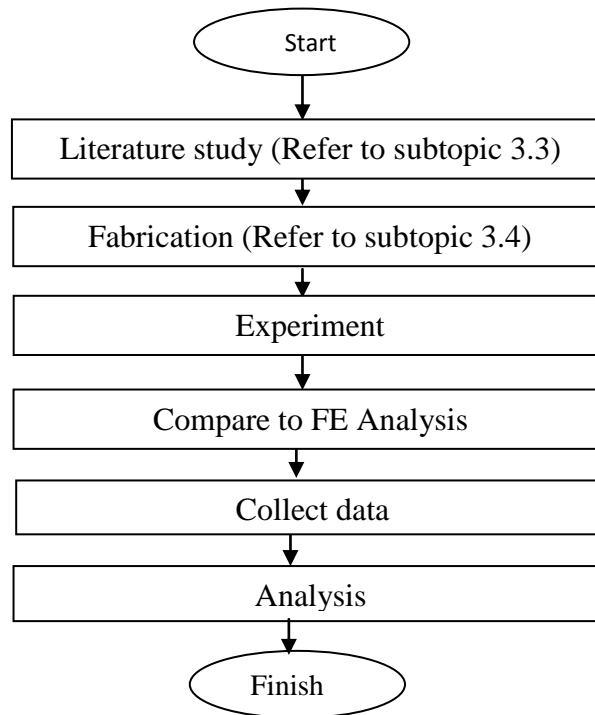


**Figure 3.1:** General flow chart

### **3.3 GATHER THE INFORMATION**

The information about this project was about the design and fabricate simple test rig for experimental and simulation study on the effect of inner span related to four point bending test. The information was collected from certain source such as internet (related journal), UMP thesis, and related person to this field.

#### **3.3.1 Information from the Internet**

The information from the internet was most important to assure non-stop information about this topic.

### **3.3.2 Information Ump Thesis and Journal**

Journal is one of important references to refer in order to get right and suitable method to perform this project especially in scope of method to do list and example to type an introduction, literature review, methodology and more. Although sometime the thesis was not related to this project title but the method is almost same. So, it's sometime useful to this project.

### **3.3.3 Information from Related Person**

The related person that was related to this project is the supervisor that guide on how to elaborate the concept of the four point bending test, how to design simple four point bending test rig likes beam, sticker and coupling. Supervisor also gives some advice and material how to write the proper report. Also related person was the other student that doing project that was related to the bending test although the major title is different. Those persons give an advice and proper method to perform the experiment. Some discussion has been held to get a best test rigs and result.

### 3.4 DESIGN AND FABRICATION

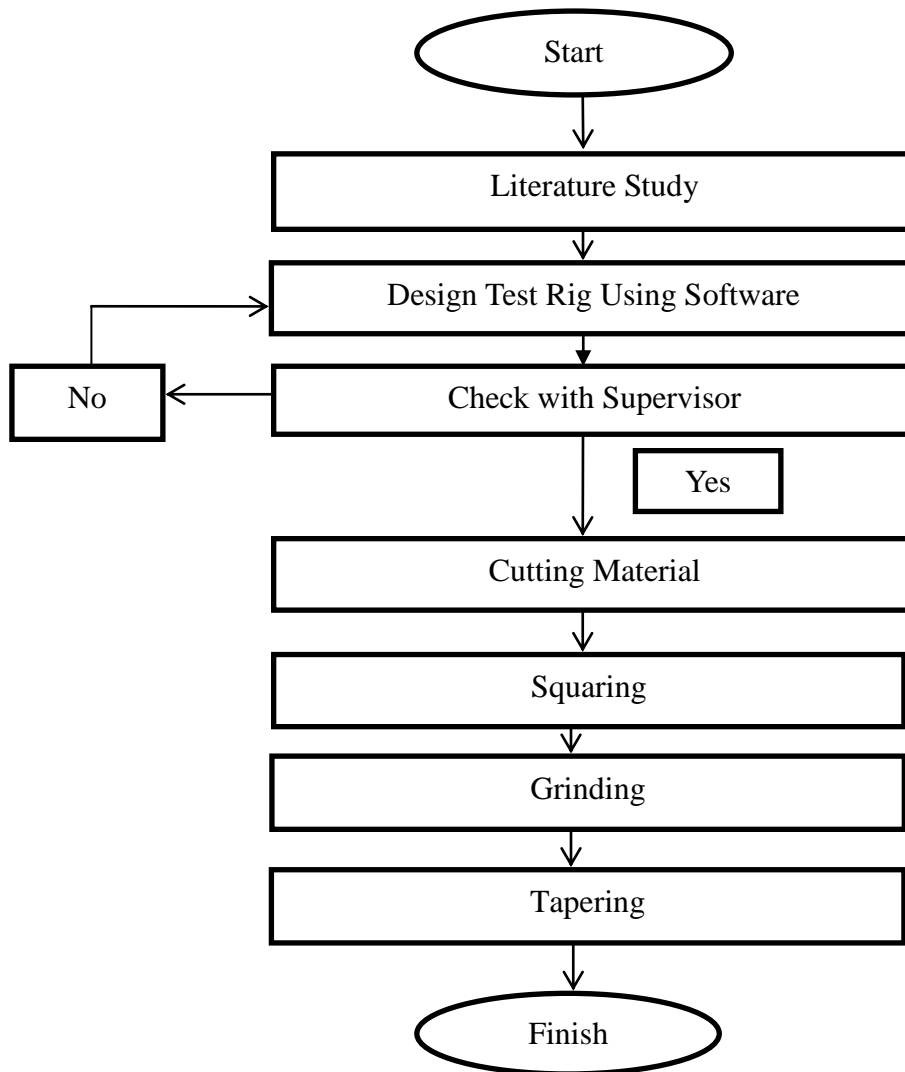
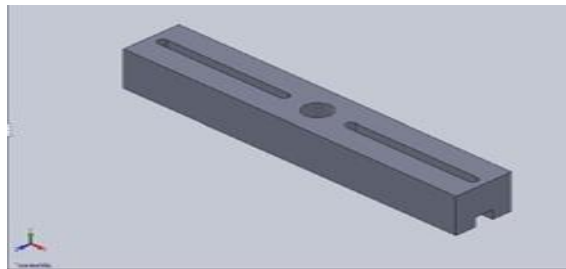


**Figure 3.2:** Fabrication flow chart

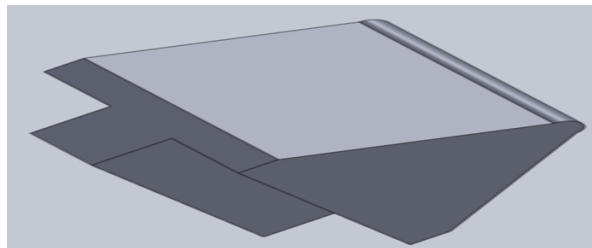
### 3.4.1 Test Rig Design

For the design test rig fixture four point bending use the Solidwork software. Solidwork is a 3D mechanical CAD (computer-aided design) program that runs on Microsoft Windows. Solidwork is a Parasolid-based solid modeler, and utilizes a parametric feature-based approach to create models and assemblies. There are 3 parts that need to be design show in figure 3.3. Full detail design of this component show at appendix

1. Beam



2. Striker



3. Coupling

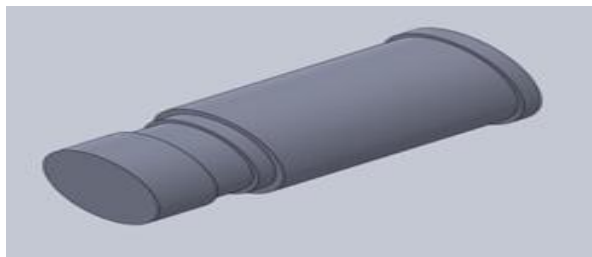


**Figure 3.3:** Design test rig four point bending test

### 3.4.2 Cutting Material

For cutting material the machine that used is bench saw. A bench saw is often utilized to split long pieces of wood lengthwise, but it can be used for shorter pieces as well. The saw blade is movable, allowing the user to adjust the angle at which the blade comes in contact with the wood. The blade can be moved up and down, thereby allowing the user to cut wood at different depths according to their needs. Figure 3.4 show benches saw cutting machine.



**Figure 3.4:** Bench saw cutting machine

### 3.4.3 Squaring Material

For this step use the conventional milling machine. Milling cutters are cutting tools typically used in milling machines or machining centers and occasionally in other machine tools. They remove material by their movement within the machinery directly from the cutter's shape. Figure 3.5 show the conversional milling machine.





**Figure 3.5:** Milling machine

#### **3.4.4 Grinding**

A grinding machine, often shortened to grinder, is a machine tool used for grinding, which is a type of machining using an abrasive wheel as the cutting tool. Grinding is used to finish work pieces which must show high surface quality (e.g., low surface roughness) and high accuracy of shape and dimension. For this project, I used the grinding machine for surface finish. Figure 3.6 show the grinding machine.



**Figure 3.6:** Grinding machine

### 3.4.5 CNC Software / Mastercam

Before do the cutting part, we need to draw the design by using Mastercam. Mastercam's comprehensive set of predefined tool paths which including contour, drill, pocketing, face, peel mill, engraving, surface high speed, advanced multiaxis, and many more and enable us to cut parts efficiently and accurately.



**Figure 3.7:** Mastercam software

### 3.4.6 Tapering

Process fabricate the fixture continue by using Electric discharge machining (EDM) wire cut. Wire-cut EDM is typically used to cut plates as thick as 300mm and to make punches, tools, and dies from hard metals that are difficult to machine with other methods. Wire-cutting EDM is used when low residual stresses are desired, because it does not require high cutting forces for removal of material. For this project, it used to produce taper angles of up to  $\pm 30^\circ$  and R2 at edge of the striker. Figure 3.8 show the wire-cut machining.



**Figure 3.8:** Wire-cut EDM

### 3.4.7 Turning

Turning is a form of machining, a material removal process, which is used to create rotational parts by cutting away unwanted material. The turning process requires a turning machine or lathe, workpiece, fixture, and cutting tool. Turning is used to produce rotational, typically axial-symmetric, parts that have many features, such as holes, grooves, threads, tapers, various diameter steps, and even contoured surfaces.



**Figure 3.9:** Lathe Machine

### 3.4.8 Complete Test Rig

A complete test rig was built by considering it compatible to suit the space area to be fitted inside the Shimadzu machine. On these requirements, the completed 4PBT test rig was designed and fabricated as shown in Figure 4.7. Size of the fabricated test rig is 300mm length x 50 mm width x 40 mm height for beam, 50mm length x 50 mm width x 40 mm height for striker and is 70mm length with radius 32mm for coupling.

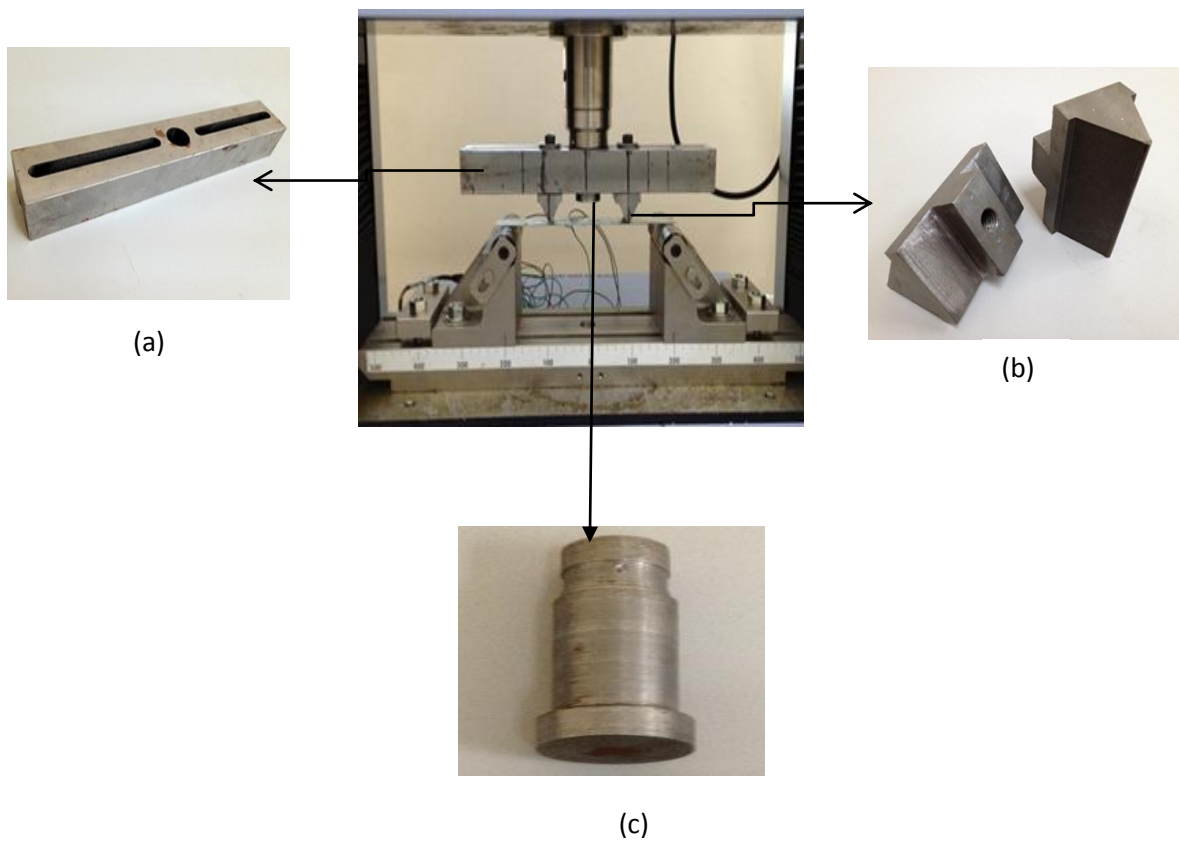


**Figure 3.10:** Design consideration in test rig fabrication

### 3.5 FOUR POINT BENDING TEST

#### 3.5.1 Specimen Preparation

##### 3.5.1.1 Shearing Machine

Shearing force machine had been used in this project to cut the thin wall material or sheet metal for the purpose of covering the main structure of the experimental test equipment. The galvanized steel need to be cut into specimen according to ASTM Standards, which the raw material of galvanized steel need to be cut into a rectangular size of 220mm x 30mm x 1mm by using shearing bench saw.



**Figure 3.11:** Shearing Bench Saw



**Figure 3.12:** Plates of galvanized steel (220mm x 33 mm x 1mm)

### 3.5.1.2 Strain Gauge

While there are several methods of measuring strain, the most common is with a strain gage, a device whose electrical resistance varies in proportion to the amount of strain in the device. The most widely used gage is the bonded metallic strain gage.

The metallic strain gage consists of a very fine wire or, more commonly, metallic foil arranged in a grid pattern. The grid pattern maximizes the amount of metallic wire or foil subject to strain in the parallel direction (Figure 3.13). The cross-sectional area of the grid is minimized to reduce the effect of shear strain and Poisson Strain. The grid is bonded to a thin backing, called the carrier, which is attached directly to the test specimen. Therefore, the strain experienced by the test specimen is transferred directly to the strain gage, which responds with a linear change in electrical resistance. Strain gages are available commercially with nominal resistance values from 30 to 3,000  $\Omega$ , with 120, 350, and 1,000  $\Omega$  being the most common values.

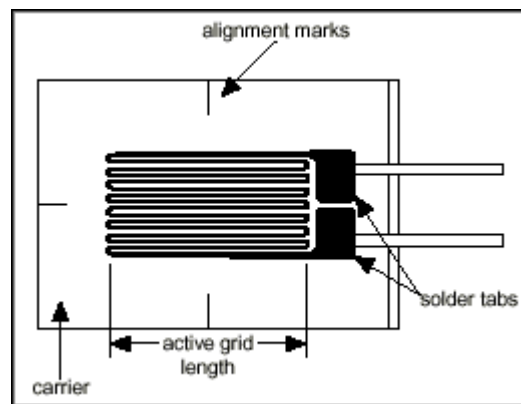


**Figure 3.13:** Bonded metallic strain gage



### 3.5.2 Test Setup

The tests were performed using a 100kN Shimadzu tension/compression machine. The machine is computer controlled with the ram movement is controlled from the control panel. The test rig was properly aligned on the Shimadzu machine by clamping onto the base at the center place of the test machine. The experimental setup used for the 4PBT is shown in Figure 3.14 to figure 3.16



**Figure 3.14:** Four point bending test setup



**Figure 3.15:** Strain connected to data logger



**Figure 3.16:** Data logger connected to laptop

For data collection, there are two data acquisition systems have been used in this experiment i.e. from the machine and PC-based a data acquisition system (DAQ). The data from the machine's DAQ is used to gather the bending speed during the 4PBT. Meanwhile, PC-based DAQ is purposely used for measurement of strain on the workpiece during the process. Strain gauge location on the specimen was show in figure 3.17.

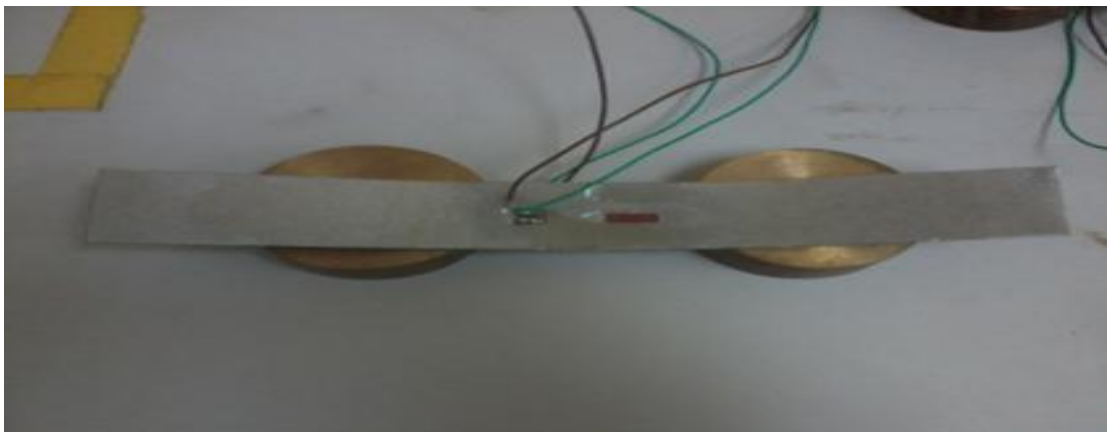


**Figure 3.17:** Strain gauge location on specimen during 4PBT

There are a total of 9 specimens were used in this investigation. Specimens that used for this research is galvanized steel. In each process setting, three specimens have been used. For specimen preparation, the 1 mm thick in-received galvanized steel were cut



with a shearing machine to the specified workpiece size 220 mm x 33 mm. Among the consideration in cutting the workpiece is to standardize the workpiece width at 33 mm to accommodate plane strain analysis condition as implemented in the finite element analysis. All workpiece were marked on the sidewall to confirm a right setting during the bending process. Strain value was measured with a PC-based DAQ by using strain gauge. Strain gauges were spot welded at selected locations on the workpiece as shown in Figure 3.17. The signals were converted from analogue to digital by NI's data logger connected to the laptop.

### 3.5.3 Test Procedure

A total of three experiments were conducted on nominally identical workpiece where the centre line was located within the focal line region as shown in Figure 3.18. Initially, the used inner was 100mm and outer spans were fixed at 200 mm respectively. The test condition was changed with different inner span to 120mm and 140 mm.

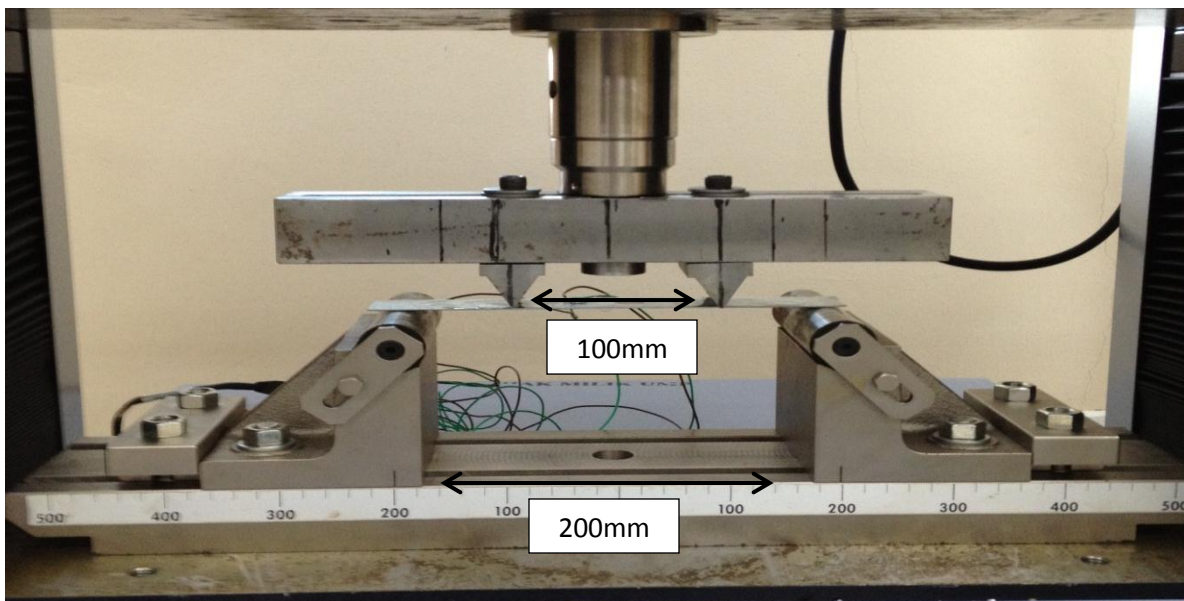


**Figure 3.18:** Specimen positioning inside the test rig during 4PBT

There are three main steps was set during the 4PBT. Initial setting had been done before the actual test was commenced. The workpiece with strain gauge ready were placed on the bending support. The machine ram was moved down to make an initial contact between the striker and workpiece top surface. Most importantly, the centre section of the blank must be positioned exactly at the middle between both of the bending supports. Displacement of striker in right and left must be same from the center.

The complete experiments were conducted in the following steps:

Step 1- The workpiece with strain gauge ready were placed on the bending support. Striker was set up 100mm and the support was fixed at 200mm. The stroke limit was setup fixed at 30mm from the center of the beam.

Step 2- It was followed by setting at the pc used the trapezium x software. In addition workpiece was connected to the data logger used the DasyLab software at the laptop.

Step 3- The final step was used for the four point bending process. The striker movement was calculated based on the plotted curve. In this experiment, the bending speed has been specified at 1 ms<sup>-1</sup>. Make sure run the four bending process from the press machine and DasyLab software from the laptop simultaneously.

### 3.6 EXPERIMENTAL AND SIMULATION FLOW CHART

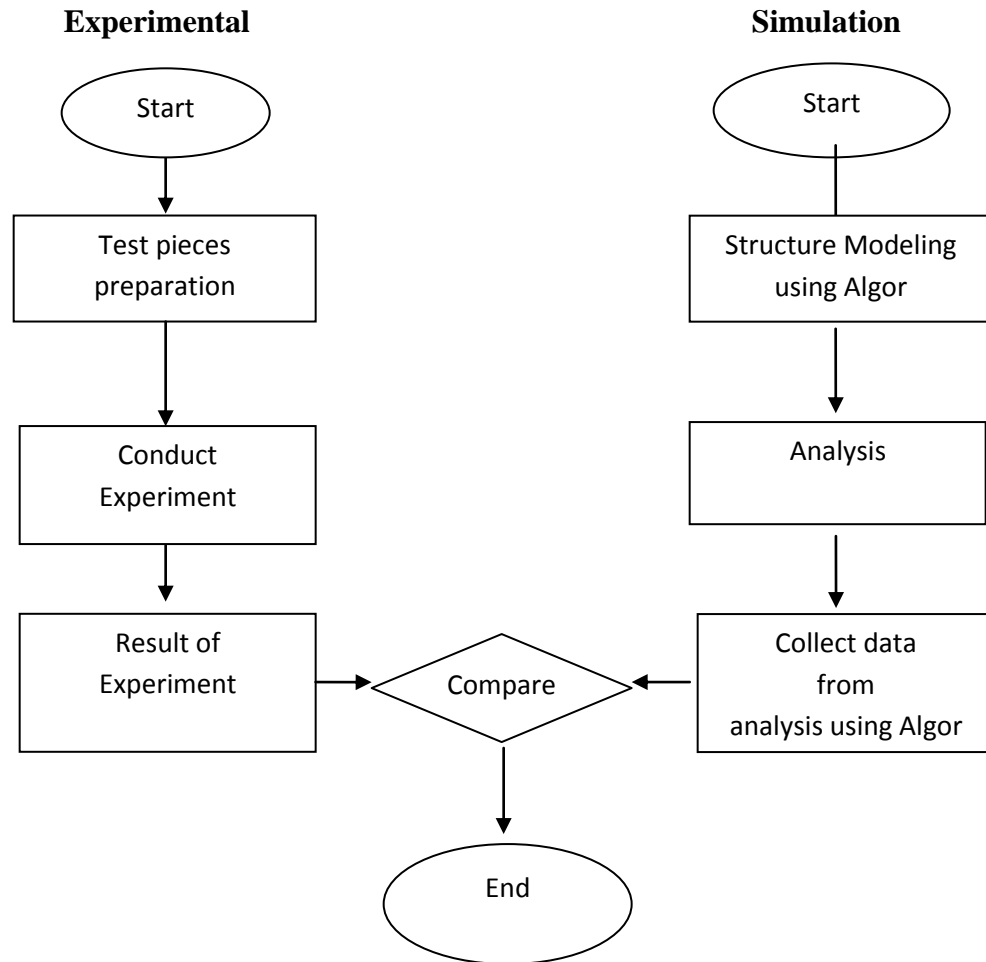
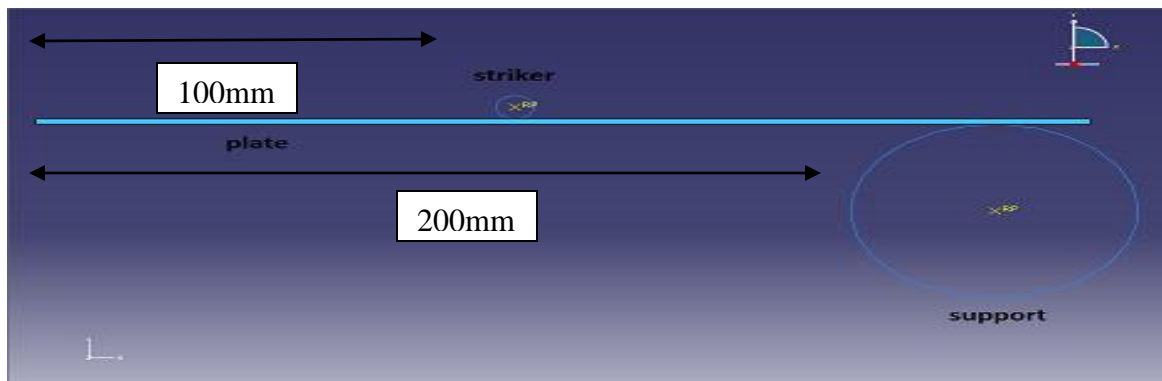


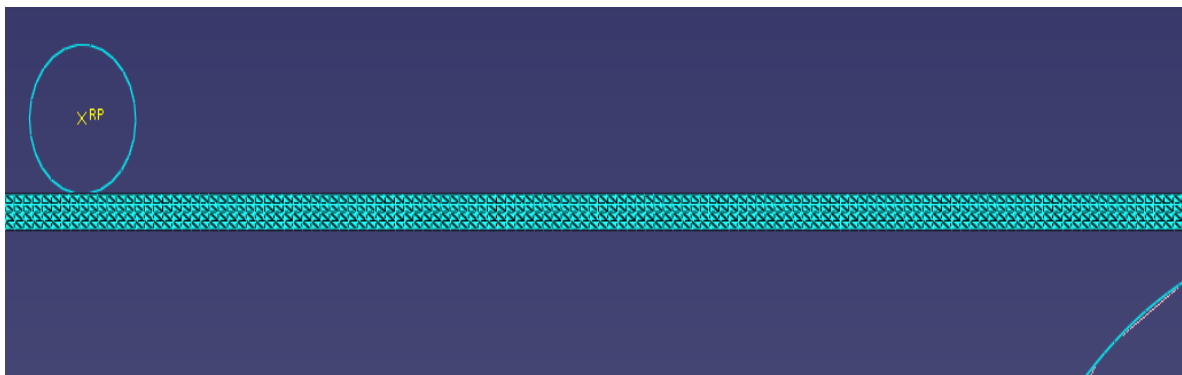
**Figure 3.19:** Experiment and simulation flow chart

### 3.7 FINITE ELEMENT MODEL FOUR POINT BENDING

The main objective of this analysis is to investigate the reliability of all the material properties and setting parameters of the studied system. From this task, it able to determine reliability of all the input parameters in the finite element model based on their good agreement with the experiment results. The model was developed to compare result simulation with experimental result. The simulation condition was setup at three different cases that based on the inner span length; i.e. 100 mm, 120mm and 140mm. The geometrical and meshes of the model are shown in the Figure 3.20 (a) and (b). The same configuration will be used for the analysis at static condition.



(a)



(b)

**Figure 3.20:** (a) The geometrical model for 4PBT (b) The meshed model for simulation

The present analysis involves implicit ABAQUS methods. The implicit solution algorithm applied for the plain strain logarithm. First step of this analysis concentrates on determination of the strain distribution inside the workpiece. The implicit method was adopted for easy to run the simulation. Since then, the plane strain method based implicit algorithm was the most suitable solution to generate data in the fastest time. In the plane strain analysis, continuum four point element (C4PE) has been adopted.

### **3.7.1 The Material Properties**

In developing the finite element model, the workpiece was assumed as a continuum body, isotropic and homogeneous which represent the condition of the material properties do not vary with direction or orientation and identical properties at all points. The material specifications for the current analysis were obtained from the references and the experiment results. The full details of the material properties and their source of reference can be found in the Appendix E.

### **3.7.2 Boundary Condition**

In addition the fundamental material characteristic, the other input parameters must be defined to complete the model. Among the important input parameters are an initial condition and interaction properties. The initial settings for the model were set based on suitability of the model in respect to the actual test conditions. Meanwhile, the interaction properties were mainly obtained from the related references from the other research studies. In the implicit analysis, different process setting was used to comply with their process requirements.

### **3.7.3 Process step**

Bending stage: The simulation has been carried under different inner span. The displacement of the rigid striker which has been used to push the workpiece downward metal plate were set equivalent to the inner span distance

## **CHAPTER 4**

### **RESULT AND DISCUSSION**

#### **4.1 INTRODUCTION**

This chapter is showing the results from the experimental and finite element analysis of four point bending test of galvanized steel. In the experiment, the sheet metal were welded by the strain gauge and connected to the data logger to get the value of strain. In addition experimental for four-point bending test used the galvanized steel without welded by the strain gauge to get value of displacement after bend. For the simulation, Abaqus software was used to get result for comparison with experimental result.

#### **4.2 FOUR POINT BENDING TEST RESULT**

For this section will show result four point bending test from the experimental. For this section there are two cases or experiment will be show as a result for this research. First case is to find strain value of four point bending test with three different inner spans. For second case is to find length specimen bend after bending test process. Strain value was taken in 1 second

### Case #1: Strain value of galvanized steel

One main purpose of this experimental work is to find the strain value in four-point bending test. It will be used as comparison to the finite element simulation output. Based on identical process output from the both analysis methods, reliability of the input parameters in the finite element model can be validated. Figure 4.1 and figure 4.2 below was shown condition before and after bending process.

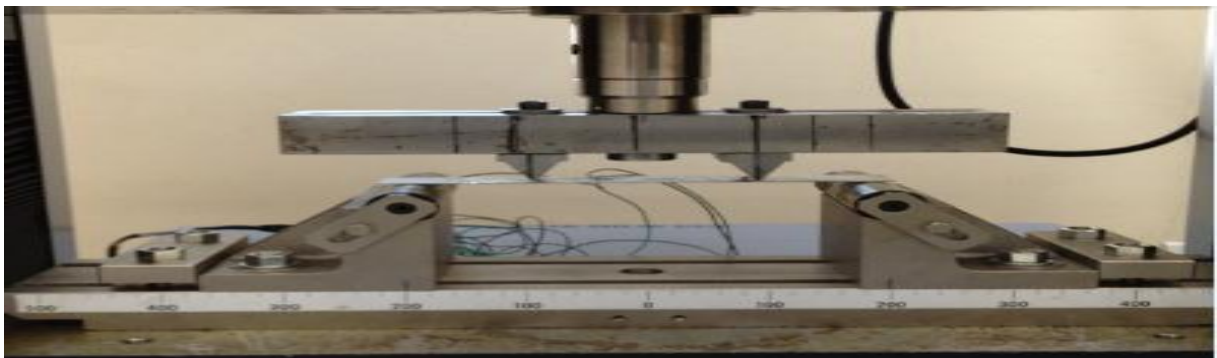


**Figure 4.1:** Condition specimen before bending process

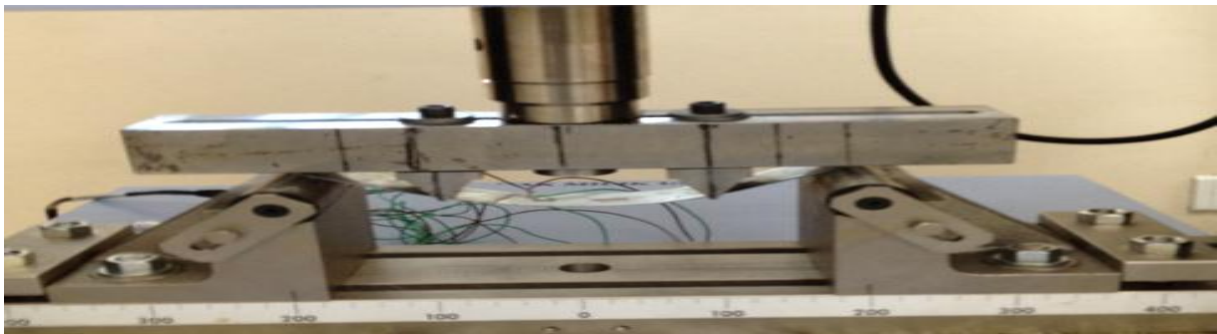


**Figure 4.2:** The bended workpiece from inner span 100mm.

Based on the four point bending test above, the time-strain graph can be plotted. The graph can be plotted by using the engineering strain. Figure 4.3 to figure 4.5 below

shown times-Strain graph for galvanized steel material having a thickness of 1.0mm with different inner span. The data of strain value was shown at the appendix C.

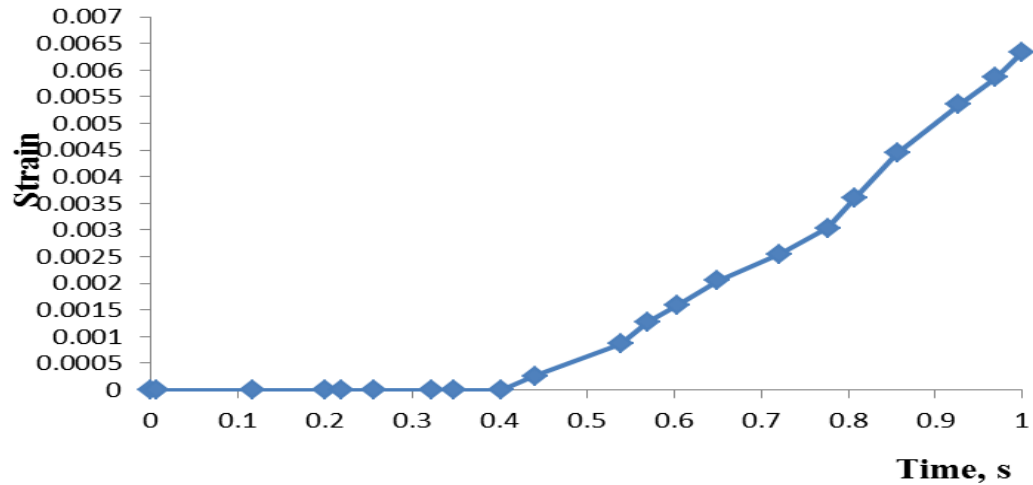


**Figure 4.3:** Graph times versus strain value for inner span 100mm

From the graph, time versus strain value graph above, the maximum strain for experiment inner span 100 mm is 0.006335. In addition, from time 0s to 0.4s the strain value for this condition is zero. Then value of strain increase with time until the four-point bending test finish.

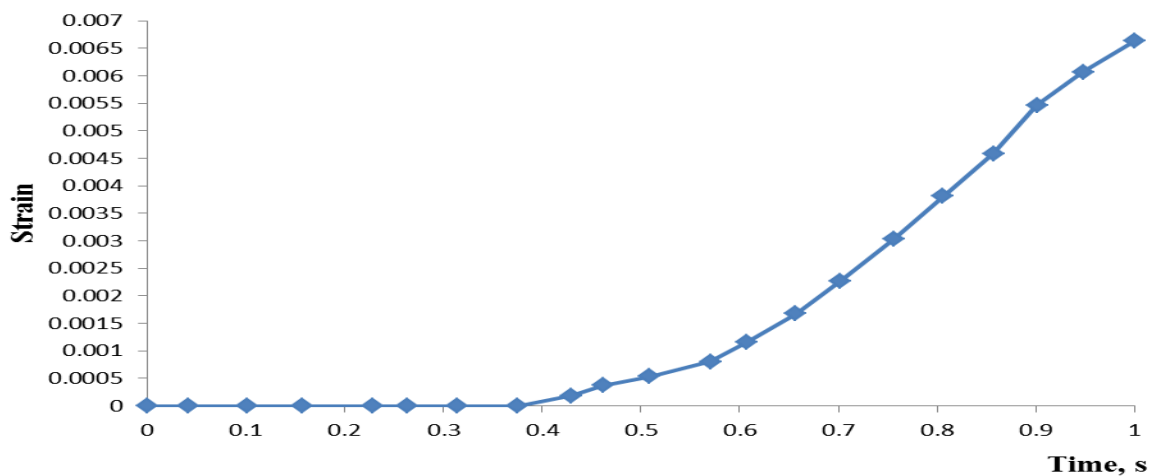


**Figure 4.4:** Graph times versus strain value for inner span 120mm



From the graph, time versus strain value graph above, the maximum strain for experiment inner span 100 mm is 0.006633. For this condition value of strain is zero from 0 to 0.37s.

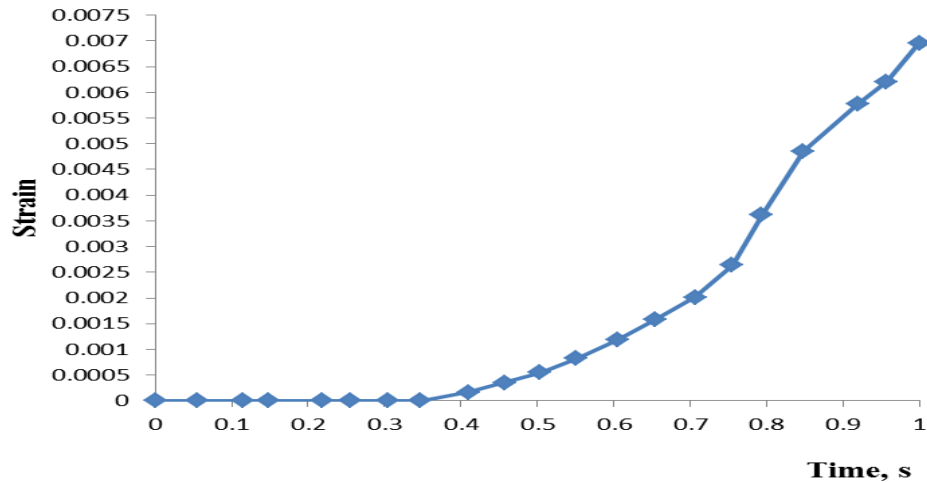


**Figure 4.5:** Graph times versus strain value for inner span 140mm

From the graph, time versus strain value graph above, the maximum strain for experiment inner span 100 mm is 0.0069626. For this condition value of strain is zero from 0 to 0.34s.

#### Case #2: Four point bending test

The second case of this experimental work is to find length of displacement after bending test process. The basic arrangement is similar to first tests but different is specimens for this case not use strain gauge. This experimental result will be used as comparison to the finite element simulation output. Based on identical process output from the both analysis methods, reliability of the input parameters in the finite element model can be validated. Figure 4.6 and figure 4.7 below was shown condition before and after bending process.

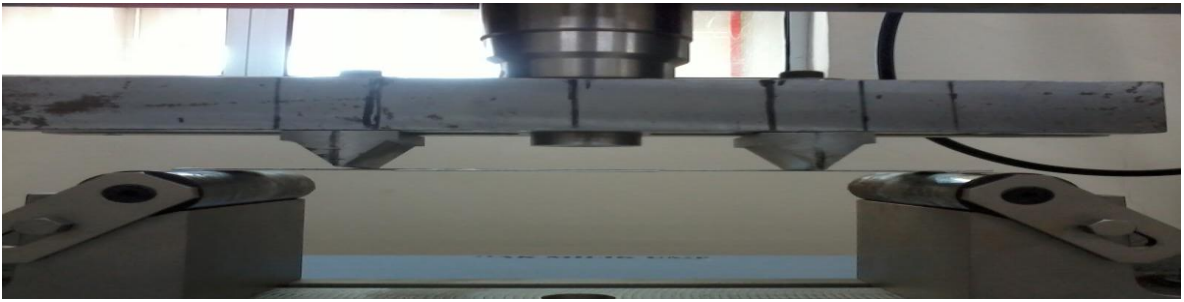


**Figure 4.6:** Condition specimen before bending process for free bend

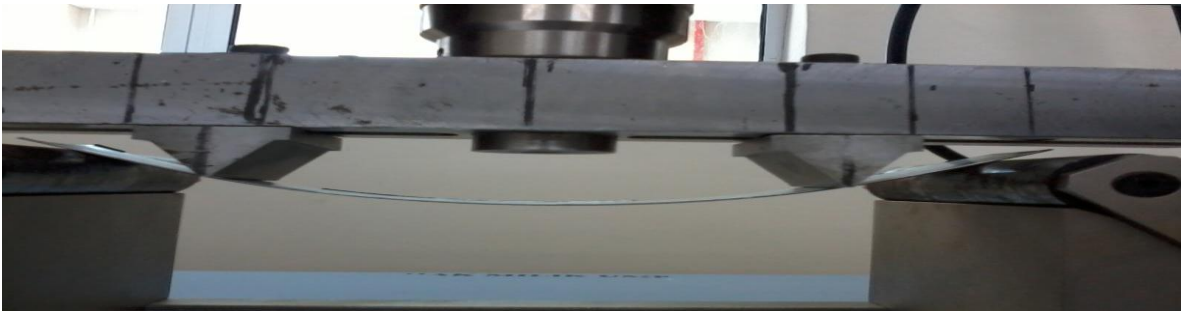
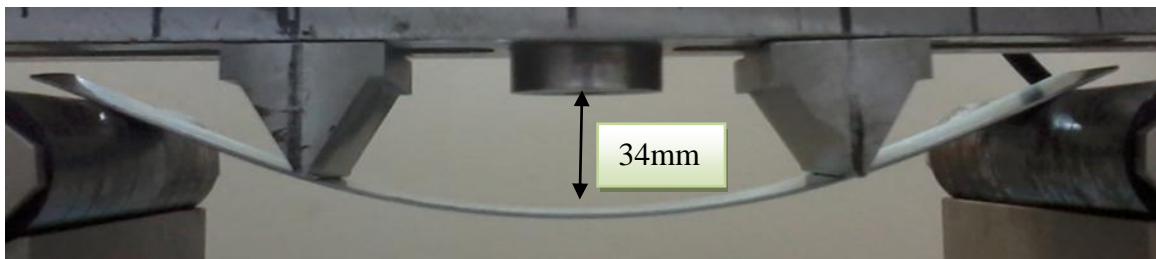
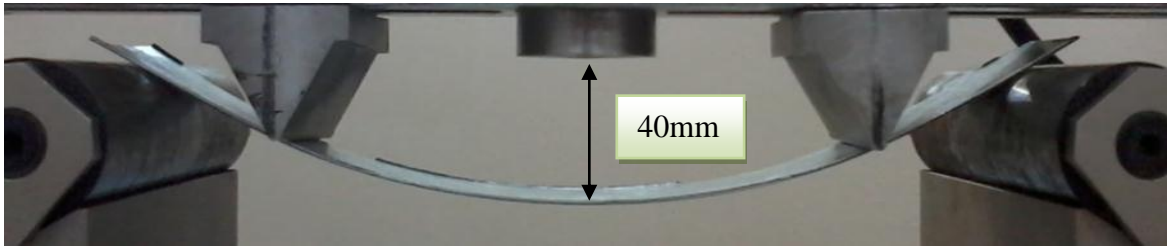


**Figure 4.7:** Condition specimen after bending process

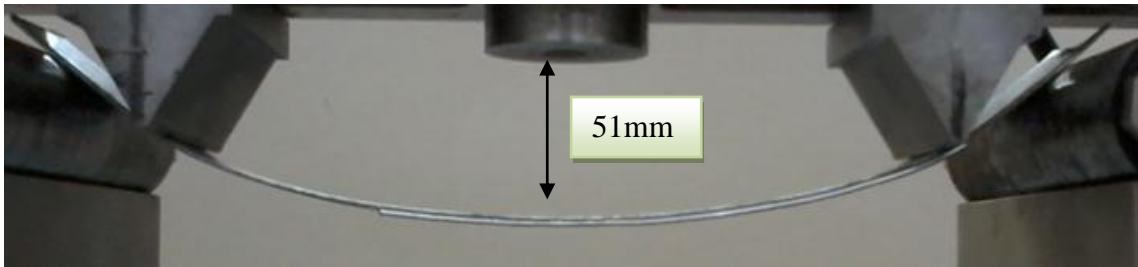
The four point bending test outputs for the three inner span setting conditions are shown in figure 4.8.



(a) Inner span = 100mm



(b) Inner span = 120mm



(c) Inner span = 140mm

**Figure 4.8:** (a) inner span = 100mm, (b) inner span = 120mm, (c) inner span = 140mm, result experimental for free bending

As can be seen above, it shows how the bending configuration has an obvious effect on the stress evolution during the four-point bending process. The specimen with the biggest inner span 140 mm has maximum length.

### 4.3 FINITE ELEMENT SIMULATION RESULT

The elastically - driven change of shape of sheet metal have been simulated with ABAQUS code. Due to plane symmetry, only half of the process was modeled (Figure 4.9). The problem consists of the surface contact between steel blank strip and the tools such as the support and striker that is a basic aspect of the stamping operations. The tools can be modeled as rigid surfaces because they are much stiffer than the blank. Figure 4.9 shows the basic arrangement of the components considered in FEM model.

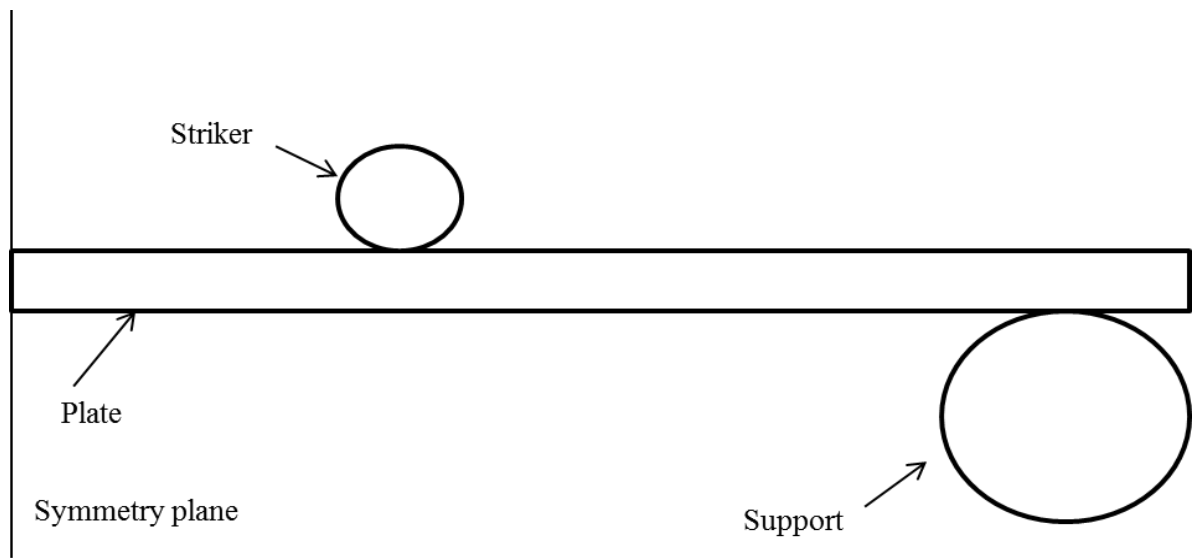


**Figure 4.9:** Geometrical description of the simulation model

### 4.3.1 Simulation of Four Point Bending

For this topic shown how process simulation for four point bending test was doing. It can see in figure 4.10 to figure 4.12.

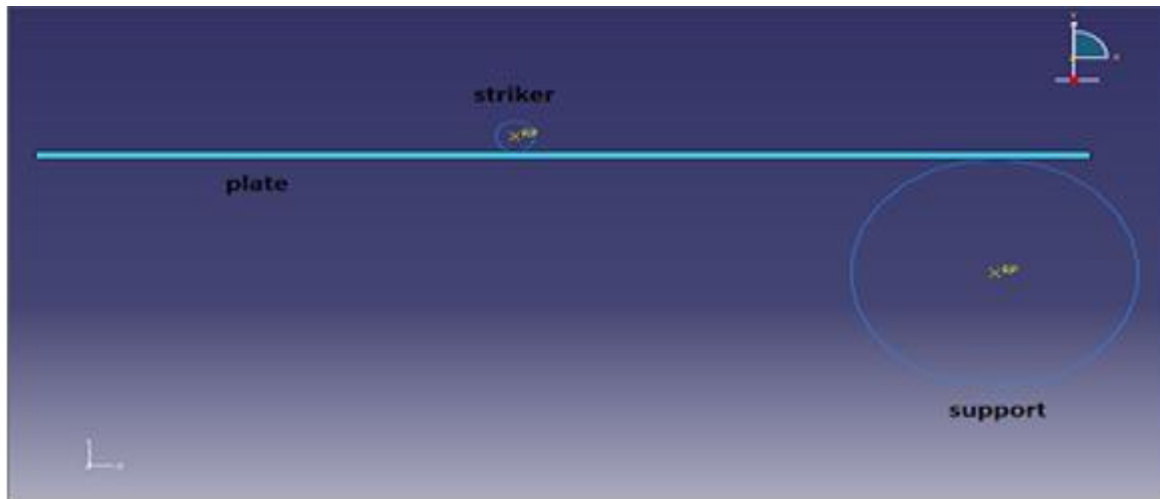


**Figure 4.10:** Striker start touching the workpiece

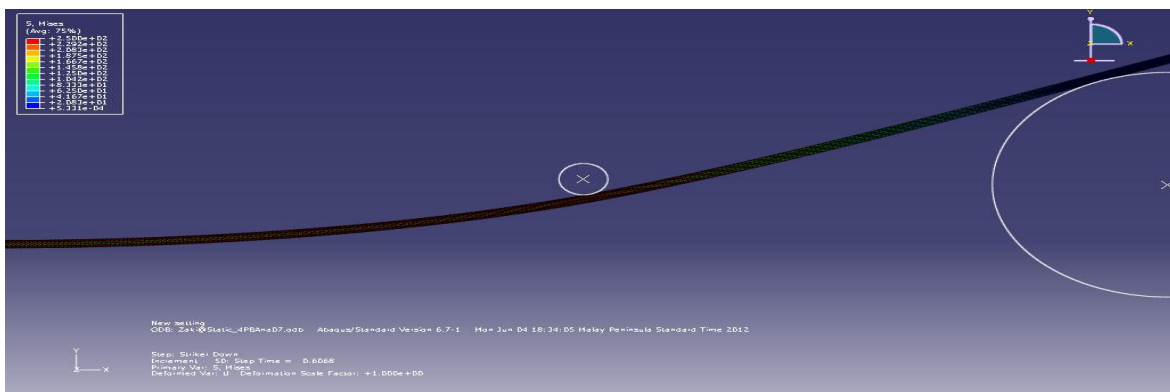


**Figure 4.11:** During bending process

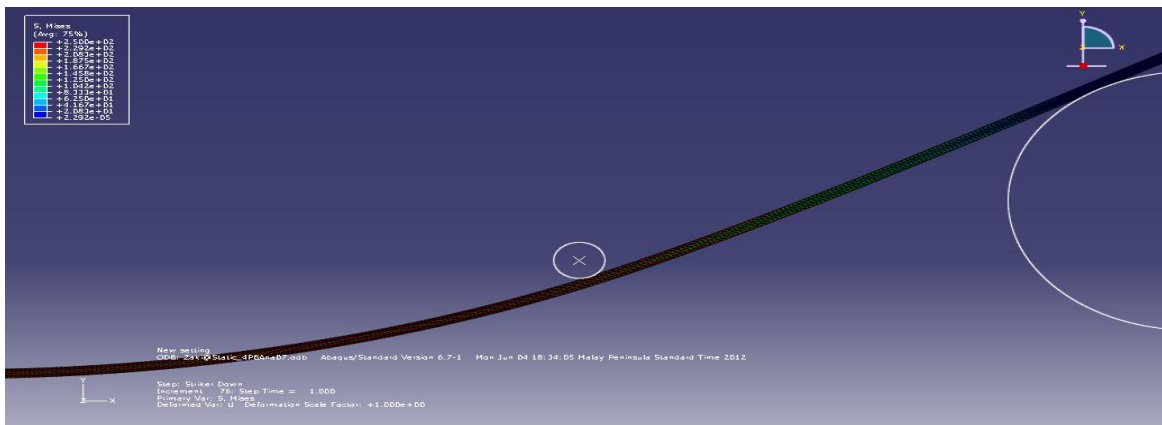
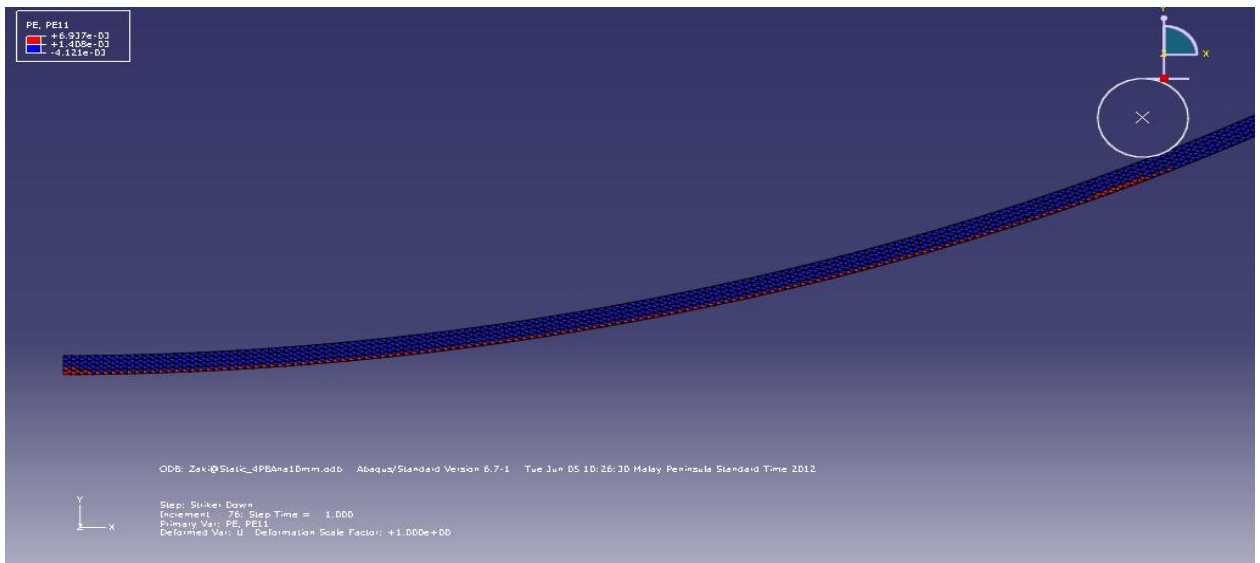


**Figure 4.12:** After bending process

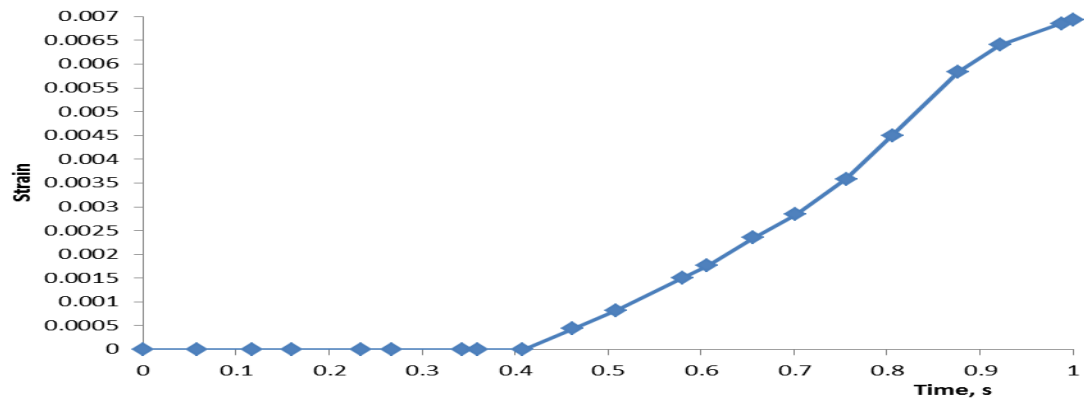
### 4.3.2 Result Simulation

#### Case #1: To find strain value

The first discussion will be concentrated on final bending output to find value of strain. Based on the simulation four point bending test above, the time-strain graph can be plotted. Figure 4.13 to figure 4.15 below shown times-Strain graph for galvanized steel material having a thickness of 1.0mm with different inner span. For this chapter also show condition strain of galvanized steel on simulation. The data of strain value was shown at the appendix D. From this graph will compare with the result from experimental and show in subtopic 4.4.



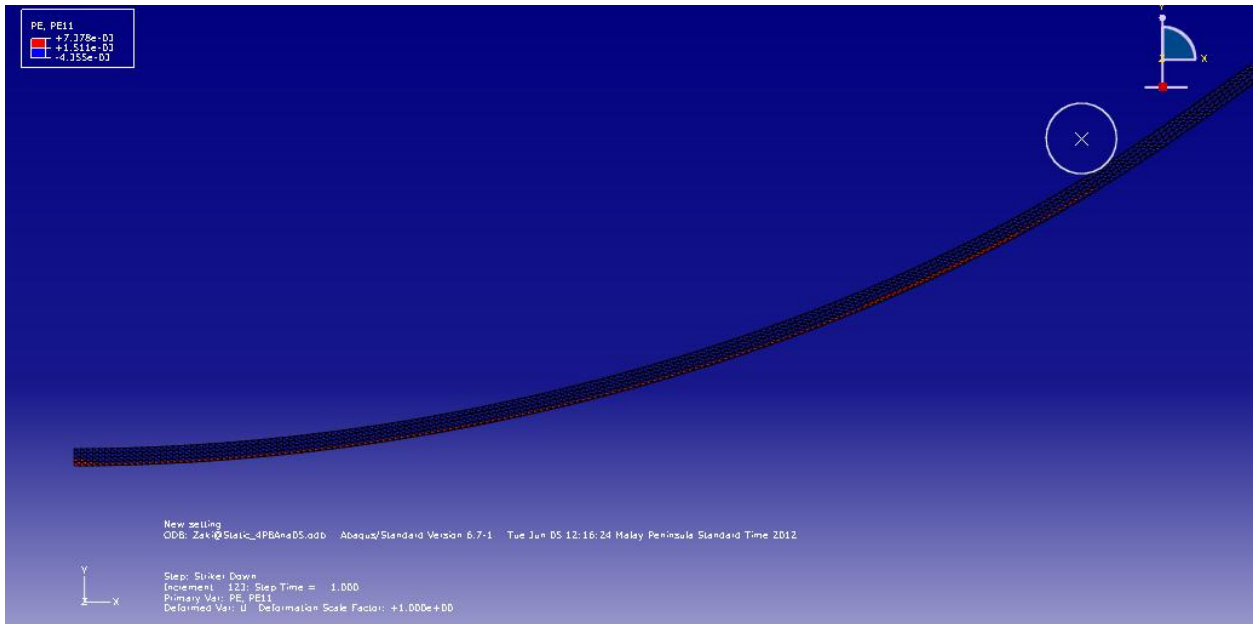
(a) Simulation inner span 100mm



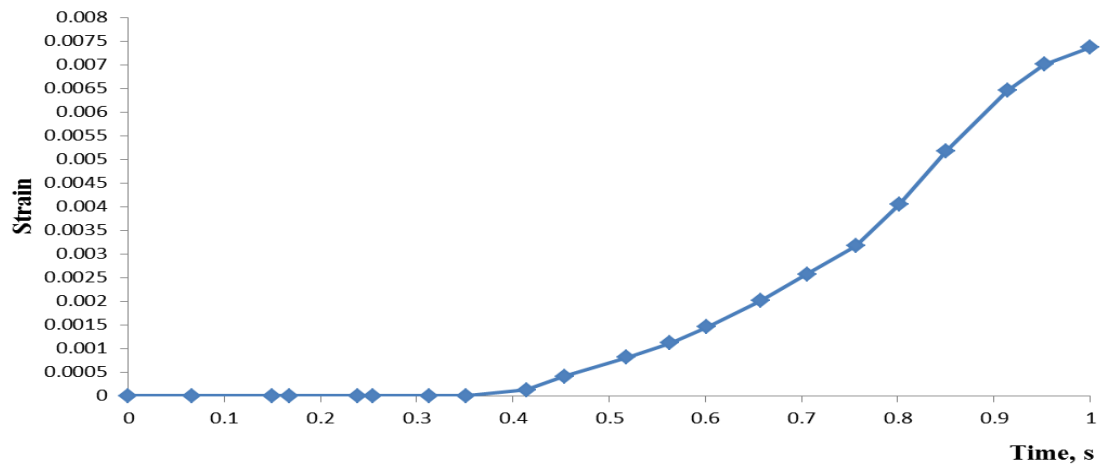
(b) Graph times versus strain value for inner span 100mm

**Figure 4.13:** Result simulation for inner span 100mm

From the graph, time versus strain value graph above, the maximum strain for experiment inner span 100 mm is 0.006937.



(a) Simulation for inner span 120mm

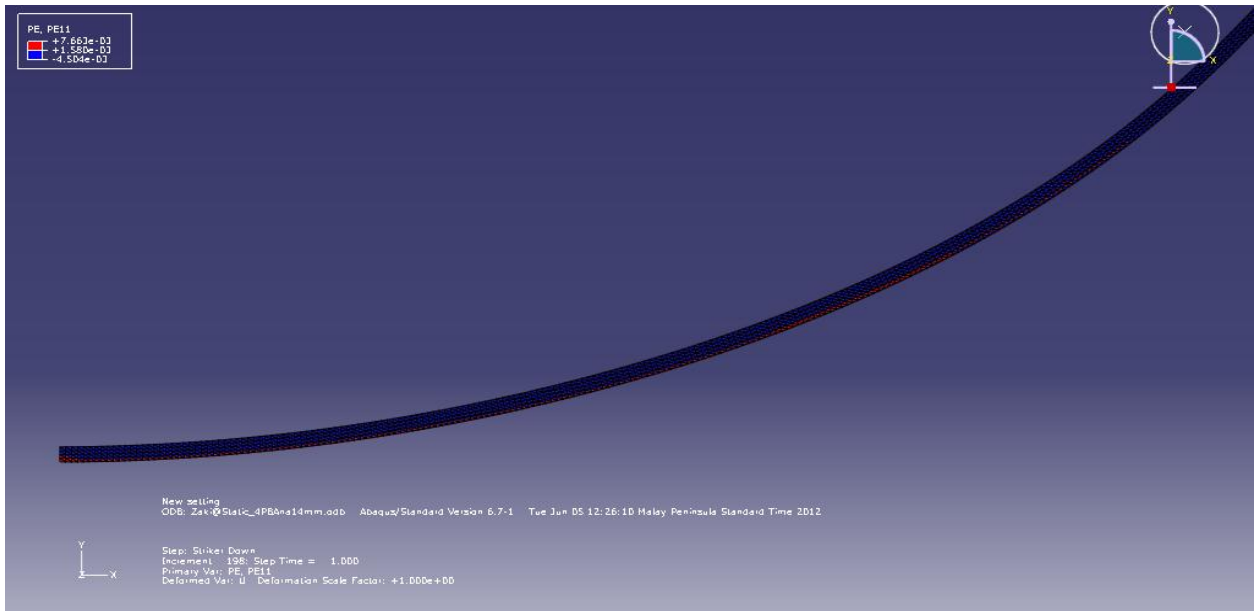


(b) Graph times versus strain value for inner span 120mm

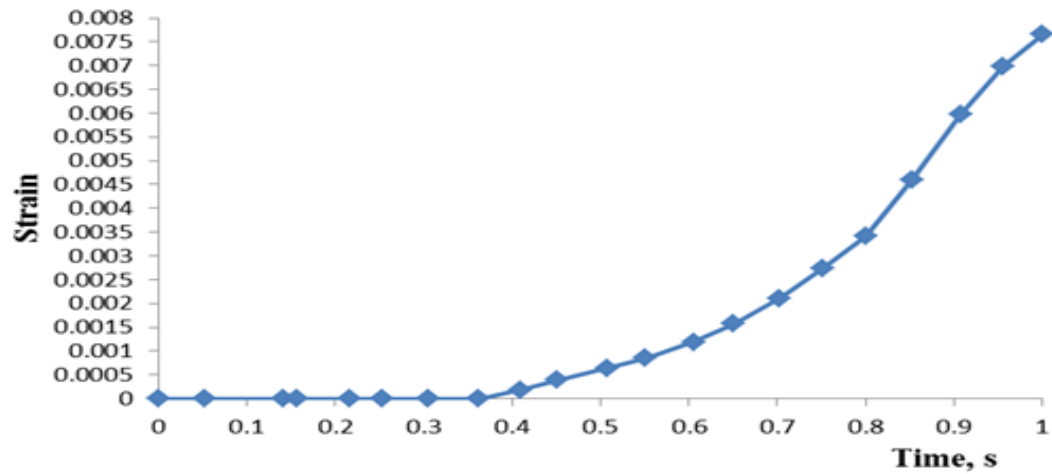
**Figure 4.14:** Result simulation for inner span 120mm

From the graph, time versus strain value graph above, the maximum strain for experiment inner span 120 mm is 0.007366.





(a) Simulation for inner span 140mm



(b) Graph times versus strain value for inner span 140mm

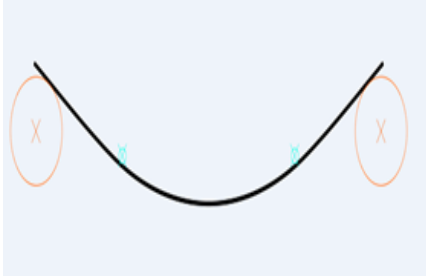
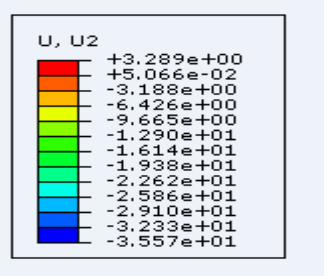
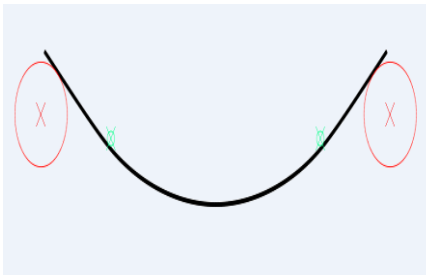
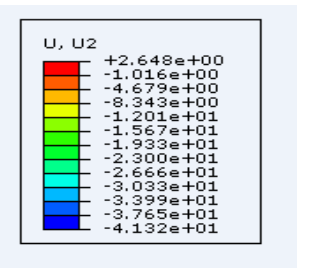
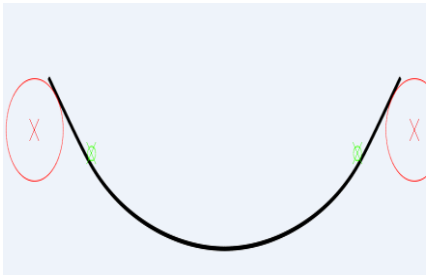
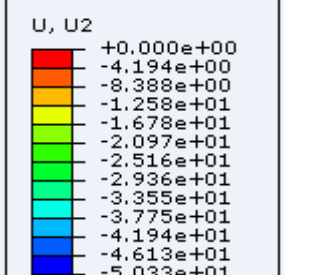
**Figure 4.15:** Result simulation for inner span 140mm

From the graph, time versus strain value graph above, the maximum strain for experiment inner span 140 mm is 0.007663.

Case #2: find length displacement after bend

The second case will be concentrated on final bending output to find value of length of displacement after bending process. Based on the simulation four point bending test above, value of length will get. Condition specimen after simulation and length value for galvanized steel material with thickness of 1.0mm was shown in table 4.1. From this table will compare with the result from experimental and show in subtopic 4.4

**Table 4.1:** Result simulation

Test condition	Simulation	Length value
Inner span = 100 mm		 <pre> U, U2 +3.289e+00 +5.066e-02 -3.188e+00 -6.426e+00 -9.665e+00 -1.290e+01 -1.614e+01 -1.938e+01 -2.262e+01 -2.586e+01 -2.910e+01 -3.233e+01 -3.557e+01 </pre>
Inner span = 120 mm		 <pre> U, U2 +2.648e+00 -1.016e+00 -4.679e+00 -8.843e+00 -1.201e+01 -1.567e+01 -1.933e+01 -2.300e+01 -2.666e+01 -3.033e+01 -3.399e+01 -3.765e+01 -4.132e+01 </pre>
Inner span = 140 mm		 <pre> U, U2 +0.000e+00 -4.194e+00 -8.388e+00 -1.258e+01 -1.678e+01 -2.097e+01 -2.516e+01 -2.936e+01 -3.355e+01 -3.775e+01 -4.194e+01 -4.613e+01 -5.033e+01 </pre>

#### 4.4 COMPARISON OF FE SIMULATION AND EXPERIMENTAL

Result of value of strain for different inner span for both FE Simulation and experimental was shown in table 4.2. Graph in figure 4.16 was shown the comparison of strain value between experimental and simulation. Result of value of length displacement in simulation was compared with result for experimental and shown in figure 4.17.

**Table 4.2:** Comparison strain value experimental and finite element simulation

Inner Span	100mm	120mm	140mm
Experimental	0.006335	0.006633	0.006962
FE Simulation	0.006937	0.007366	0.00766
Percentage of error POE (%)	8.68%	9.95%	9.11%

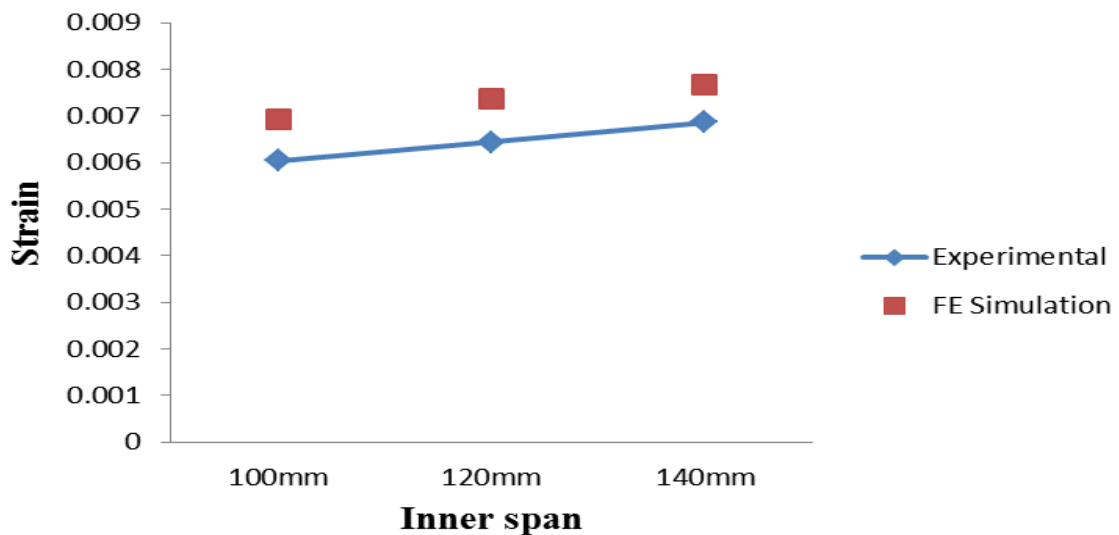
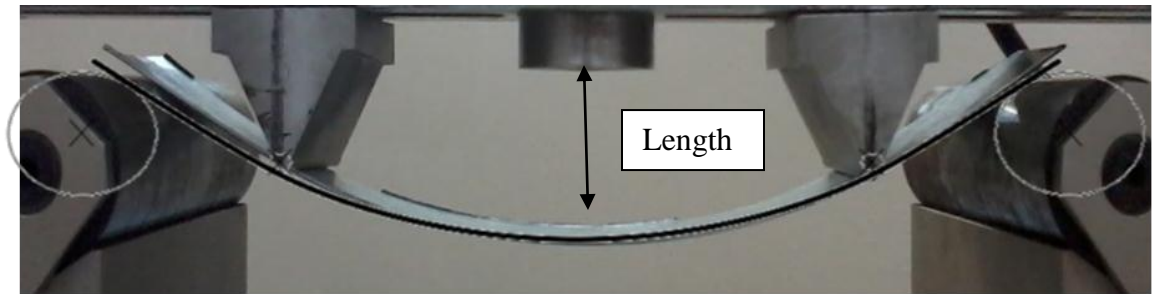
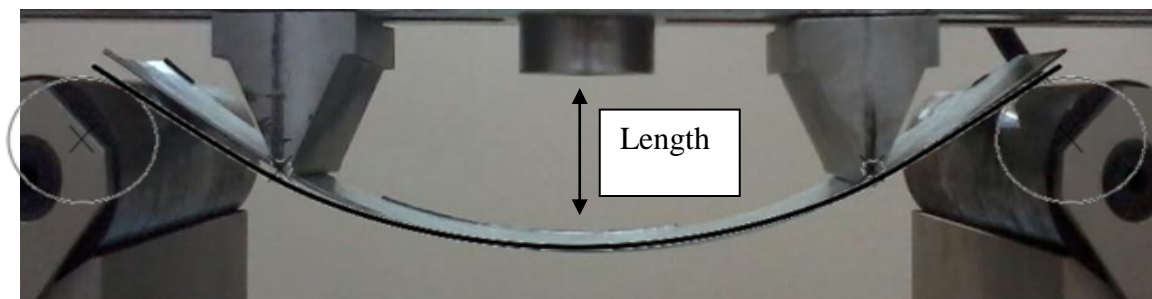


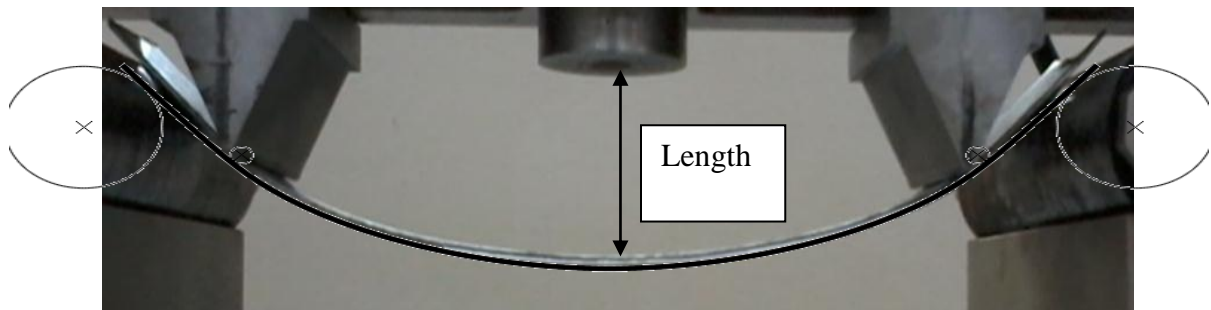
**Figure 4.16:** Graph comparison strain value experimental and FE simulation



(a) Inner Span = 100mm



(b) Inner Span = 120mm



(c) Inner Span = 140mm

**Figure 4.17:** Comparison length displacement after bend of experimental and FE simulation for inner span 100mm, 120mm and 140mm.

## 4.5 DISCUSSION

For this subtopic, it was review about discussion of result from experimental and simulation. This subtopic also discuss about comparison of simulation with experimental.

Figure 4.3 till figure 4.5 show graph strain value versus time. This experiment was conducted to the strain value high. The basic arrangement is similar to the room temperature tests with different is on an inner span. From the bending result, it shows the strain value decrease when use the higher inner span. In explaining this phenomenon, it basically caused by striker close to the support area. This because when distance striker and the support area very close will make the specimen became softer that increase possibility of part failure. An effect of the inner span during four point bending process will be explained thoroughly based on the finite element analysis.

As can be seen in figure 4.8, it shows how the bending configuration has an obvious effect on the stress evolution during the four-point bending process. The specimen with the higher inner span 140 mm was broken on the support area. This defect has been improved with smoother bending surface when smaller inner span width were adopted for the case 100 mm and 120 mm distances as shown the Figure 4.8 (a) and (b). An appropriate explanation for this phenomenon is due to evolution of stress during the four point bending process. [Cui] has emphasized in her study that the maximum longitudinal compressive stress of the four-point bending condition occurs at the contact point between the workpiece and the support tool. Therefore, tendency for part failure at the support area increases when the gap between the striker and the support is very close. This problem can be avoided by adopting bigger space between striker and supporter. The next factor that influences stress distribution is the stretching during the bending process. At the higher inner span setting, higher friction between the striker and the workpiece generate pulling force and finally broken the workpiece at the support area.

Figure 4.13 till figure 4.15 show the result research from simulation that uses 2D finite element simulation. In the 2D finite element simulation the beam become more real in the sense that it now obtains its true physical height. The width of the beam is neglected by assuming a situation of plane strain. A direct result of this more realistic representation is that the beam now physically needs to be grabbed in order to excite it. This of course will introduce larger stresses and strains at the locations where the beam is excited and constrained.

Initial observation on the bending output in the figure 4.13 till figure 4.15 verifies reliability of the developed finite element model to represent the actual four-point bending process. In all the investigated cases, it shows that the obtained result between the experiment and simulation analysis are almost identical. From the experiment, it reveals that a smaller inner span setting (100 mm) creates smaller bending moment that contributes to shorter length between the workpiece edges. In the other two cases when a bigger inner span had been adopted, the bending moment effect was reduced and finally produced bigger gap at the end of bending process.

The finite element analysis was performed to test the reliability of all the input parameters have been gathered from the experiments. It is determined by comparing the outcomes from the both simulation and experiment results. The simulated results will determine reliability of the input parameters on the finite element model.

Figure 4.16 shows the experimental and simulation effect of strain value on the different inner span of the galvanized steel for 1mm thickness. Comparing the result of the strain value for different inner span, it is noted that inner span affected the strain value. From strain value data from the simulation, by increasing the inner span, will increase the strain value. It is same with result experimental where strain value also increase when inner span increase.

From the figure 4.16, result from experimental has the lowest values than result from simulation. From FEA, values have higher values mainly because FEA analysis does not included safety factor in the calculation. For experimental, safety factor were included in their calculation. The lowest value in experimental that means that higher safety factor was included in the calculation.

From figure 4.17 shows the result experimental and effect on length displacement after four point bending process. Comparing the result of length displacement after bending process for different inner span, it is noted that inner span was effected the length. From the simulation data, by increasing the inner span, the length displacement will increase. It also same with result from experiment where length displacement after bend process increase due to inner span increase. What can conclude from this figure is value of length displacement after bend from result experiment and simulation data is almost the same.

## **CHAPTER 5**

### **CONCLUSION**

#### **5.1 INTRODUCTION**

Generally this chapter concludes the study research. Besides that, the objective is also reviewed in this chapter to determine if it achieved or not. The contribution of this study, the limitation are also been discussed in this chapter.

#### **5.2 CONCLUSION**

Based on the study, the following remarks are drawn :

1. Inner span are strongly affected the amount of strain value which increasing the inner span will increasing the strain value.
2. Inner span also was effected the length displacement after bend which increasing the inner span, the length displacement will increase.
3. Finite Element Analysis can be used to do comparison with experimental. It because result of the graphs compared are nearly the same and the percentage of errors, (POE) are less than 10 %.



### 5.3 RECOMMENDATIONS

For the improvement of the study, there are several matters can be done:

- (i) Using a variety of materials in the experiment and simulation such as are Aluminum, Stainless Steel and so on to investigate which material that have a higher strain value.
- (ii) Using different thickness for every material used to investigate the effect of strain value with fixed the striker.
- (iii) Using a variety of method of experiment and simulation such as are using different temperature to test the material.
- (iv) Study the meshing effect to predict the strain value the by using a different mesh in the simulation and choose the result that has a nearest value with the experiment.

## REFERENCES

A.B. de Morais 2009, Mode III interlaminar fracture of carbon/epoxy laminates using a four-point bending plate test.

Afred Scholz 2008, Experiences in the determination of TMF, LCF and creep life of CMSX-4 in four-point bending experiments.

A.Kucuk, 2000. Influence of plasma spray parameters on mechanical properties of yttria stabilized zirconia coatings. I: Four-point bend test. *Materials Science and Engineering*

ASTM. A 90, 1993, Standard test method for weight of coating on Zinc-coated (galvanized) Iron or steel articles, *Annual Book of ASTM Standards*, Vol. 01.06.

ASTM A653M, 2004, Standard specification for steel sheet, Zinccoated (galvanized) or Zinc-Iron alloy-coated (galvannealed) by the hot-dip process, *Annual Book of ASTM Standards*.

ASTM A 792M, 2003, Standard specification for steel sheet, 55% Aluminium-Zinc alloy-coated by the hot dip process, *Annual Book of ASTM Standards*.

ASTM D790-91. Standard test methods for flexural properties of unreinforced and reinforced plastics and electrical insulating materials,

ASTM D790M-93, Standard test methods for flexural properties of unreinforced and reinforced plastics and electrical insulating material', American Society for Testing and Materials, Annual Book of ASTM Standards,

D.Sturm et al. (1986) The behaviour of dynamically loaded pipes with circumferential flaws under internal pressure and external bending loads.

F.Mujika 2006, On the difference between flexural moduli obtained by three-point and four-point bending tests,

L. Lagunegrand Th. Lorriot , R. Harry, H. Wagnier 2006,. Design of an improved four point bending test on a sandwich beam for free edge delamination studies

L. Zheng, D. Petry, T. Wierzbicki, H. Rapp, 2005, Fracture prediction in 4-point bending of an extruded aluminum panel.

N.Coni, M.L Gipiela, A.S.C.M D'Oliveira and P.V.P. Marcondes 2009, Study of the Mechanical Properties of the Hot Dip Galvanized Steel and Galvalume®

P.F. Zhao C.A. Sun, X.Y. Zhu, F.L. Shang, C.J. Li, 2010. Fracture toughness measurements of plasma-sprayed thermal barrier coatings using a modified four-point bending method, Surface & Coatings Technology,

Pizhong Qiao, Lei Zhang, Fangliang Chen, Ying Chen, Luyang Shan., 2011, Fracture characterization of Carbon fiber-reinforced polymer-concrete bonded interfaces under four-point bending, Engineering Fracture Mechanics.

P t curtis (ed), crack test methods for the measurement of the engineering properties of fibre-reinforced plastics, royal aircraft establishment, technical report 88012, february 1988.

Roberts JC, Bao G, White GT. 1999 Experimental, numerical and analytical results for bending and buckling of rectangular orthotropic plates

Scholz A, Kirchner H, Hortig P, Granacher J, Berger C. 2000, Experience with service type strain cycling under thermo-mechanical conditions.

Sinval A. Rodrigues Junior, Jack L. Ferracane, A' Ivaro Della Bona, 2008, Flexural strength and Weibull analysis of a microhybrid and a nanofill composite evaluated by 3- and 4-point bending tests.

Sokolinsky VS, Shen H, Vaikhanski L, Nutt SR. 2003 Experimental and analytical study of nonlinear bending response of sandwich beams.

Sokolinsky VS, Shen H, Vaikhanski L, Nutt SR. 2004 Experimental and analytical study of nonlinear bending response of sandwich beams.

T.M. Chan, L. Gardner., 2008, Bending strength of hot-rolled elliptical hollow sections, Journal of Constructional Steel Research,

T.Zhai, Y.G. Xu , J.W. Martin, A.J. Wilkinson, G.A.D. Briggs, 1999, A self-aligning four-point bend testing rig and sample geometry effect in four-point bend fatigu. International journal of fatigue of fatigue

Wei Cheng Cui, Michael R. Wisnom, 1991, Contact finite element analysis of three- and four-point short-beam bending of unidirectional composites.

Y. Wang J. Bergstrom, C. Burman, 2006, Four-point bending fatigue behavior of an iron-based laser sintered material, International Journal of Fatigue

## **APPENDIX**





### APPENDIX C

Inner Span = 100mm

Times (s)	Strain
0	0
0.0075	0
0.1165	0
0.1995	0
0.2185	0
0.2555	0
0.3225	0
0.34715	0
0.40155	0
0.44035	0.000259
0.53885	0.000864
0.570508	0.001272
0.603653	0.001589
0.650452	0.002048
0.721803	0.002551
0.776561	0.003032
0.807859	0.003611
0.856507	0.004445
0.926954	0.005358
0.969036	0.005864
1	0.006335

Inner Span = 120mm

Times (s)	Strain
0	0
0.041435	0
0.10106	0
0.156705	0
0.22788	0
0.263825	0
0.31459	0
0.374635	0
0.429865	0.0001810
0.461813	0.0003697
0.50868	0.0005387
0.570808	0.0008046
0.606833	0.0011550
0.656493	0.0016733
0.701601	0.0022653
0.756292	0.0030328
0.805698	0.0038113
0.857005	0.0045888
0.901434	0.0054693
0.948078	0.0060685
1	0.0066330

Inner Span = 140mm

Times (s)	Strain
0	0
0.055865	0
0.115025	0
0.148065	0
0.218645	0
0.254825	0
0.304605	0
0.346675	0
0.409255	0.00016105
0.456465	0.00035489
0.503417	0.00054661
0.551108	0.00082265
0.604505	0.0011863
0.65348	0.0015806
0.706105	0.0020174
0.754578	0.0026384
0.793045	0.0036115
0.84765	0.0048586
0.91889	0.0057694
0.956475	0.0062068
1	0.0069626



## APPENDIX D

Inner Span = 100mm

Times (s)	Strain
0	0
0.058182	0
0.117413	0
0.159498	0
0.234463	0
0.267753	0
0.342656	0
0.359509	0
0.408488	0
0.461813	0.000441
0.50868	0.000826
0.580808	0.001511
0.606833	0.001765
0.656493	0.002348
0.701601	0.002838
0.756292	0.003587
0.805698	0.004504
0.877005	0.005838
0.921434	0.006407
0.988078	0.006854
1	0.006937

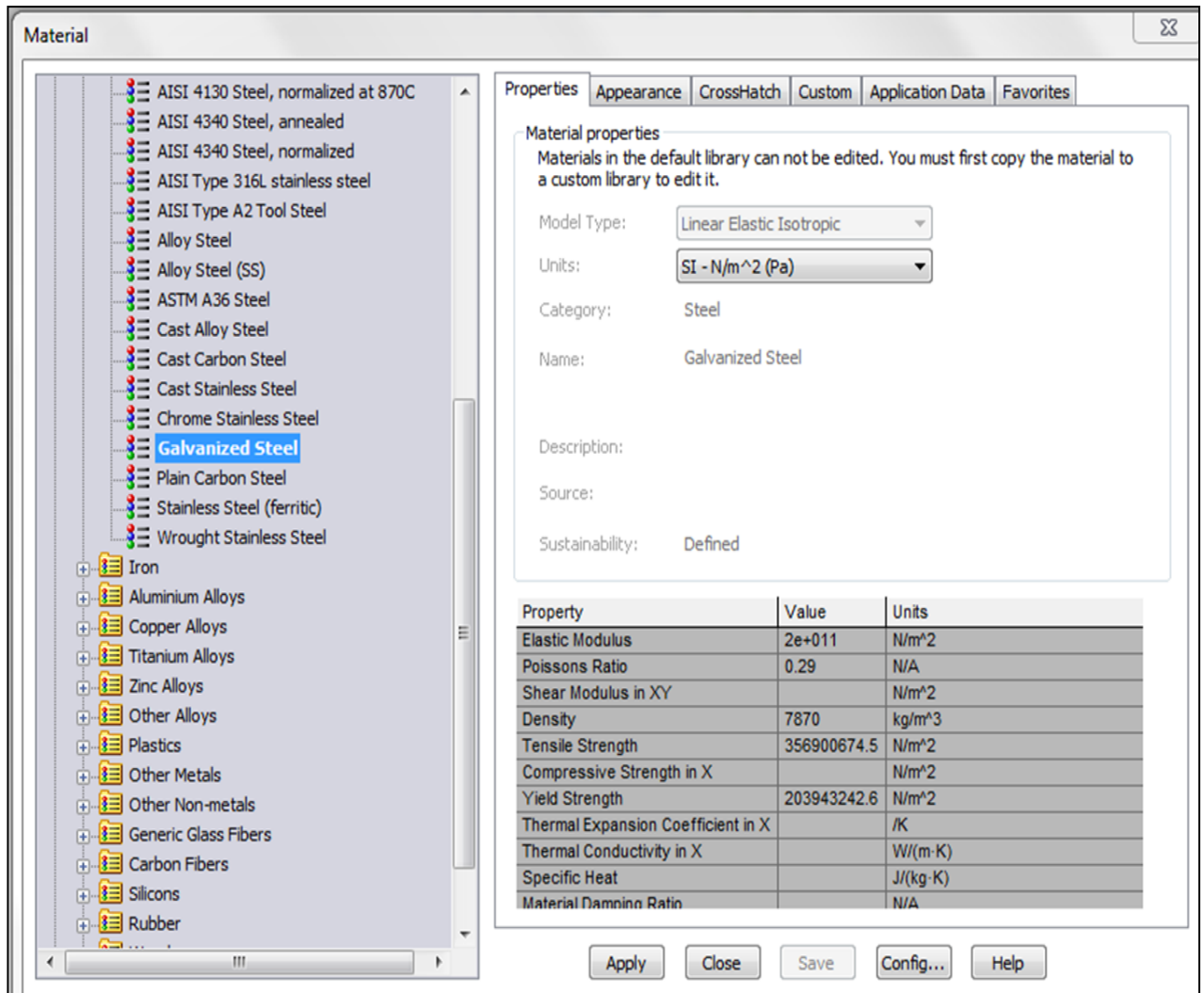
Inner Span = 120mm

Times (s)	Strain
0	0
0.052178	0
0.141025	0
0.156807	0
0.215989	0
0.253024	0
0.304637	0
0.362183	0
0.409899	0.0001810
0.451189	0.0003887
0.507904	0.0006387
0.55098	0.0008446
0.60526	0.0011880
0.650371	0.0015700
0.7028	0.0021123
0.75129	0.0027328
0.800452	0.0034113
0.851979	0.0045888
0.907282	0.0059693
0.955568	0.0069906
1	0.0076626

Inner Span = 140mm

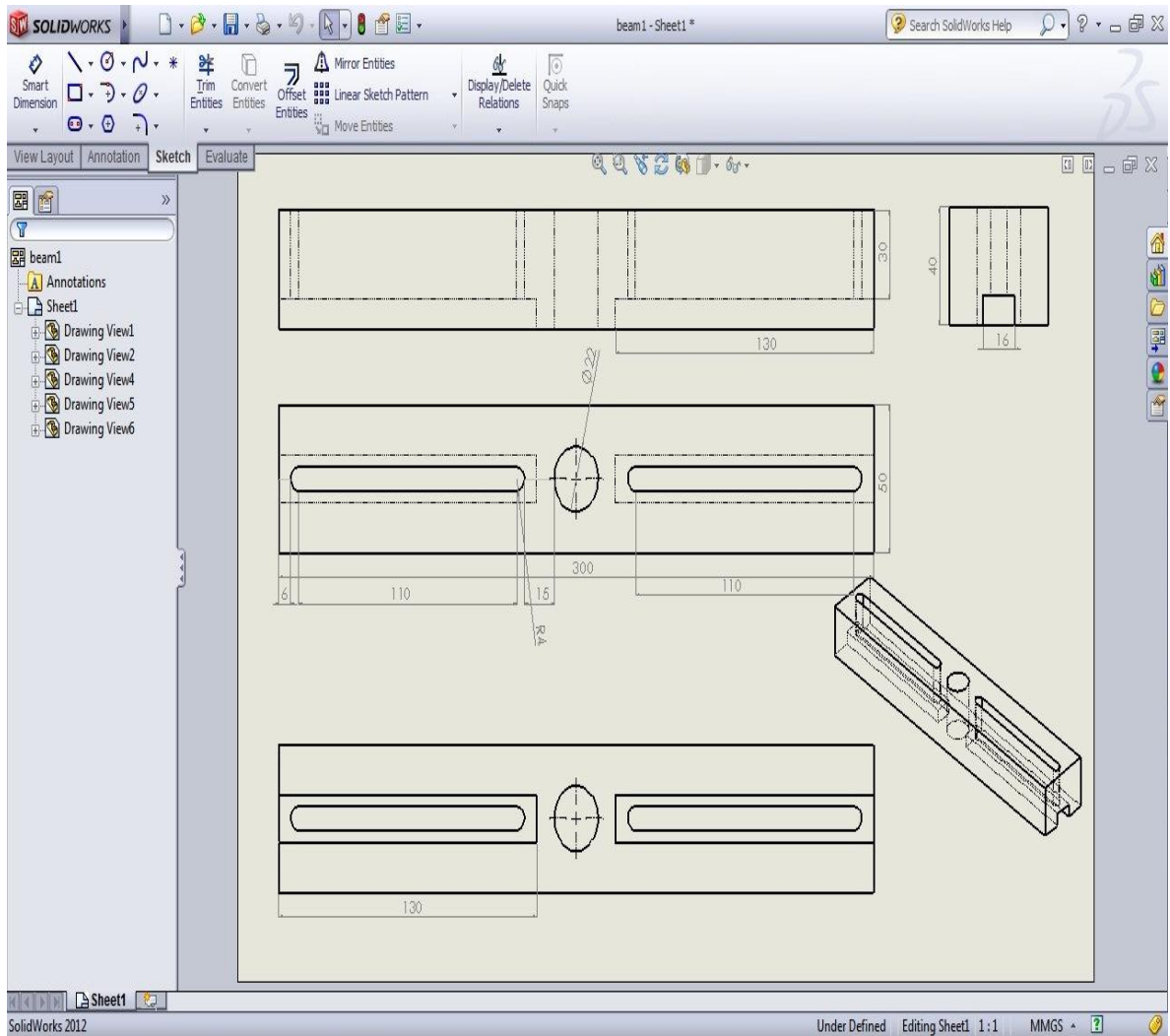
Times (s)	Strain
0	0
0.052178	0
0.141025	0
0.156807	0
0.215989	0
0.253024	0
0.304637	0
0.362183	0
0.409899	0.0001810
0.451189	0.0003887
0.507904	0.0006387
0.55098	0.0008446
0.60526	0.0011887
0.650371	0.0015706
0.7028	0.0021129
0.75129	0.0027328
0.800452	0.0034113
0.851979	0.0045888
0.907282	0.0059693
0.955568	0.0069906
1	0.0076626

## APPENDIX E

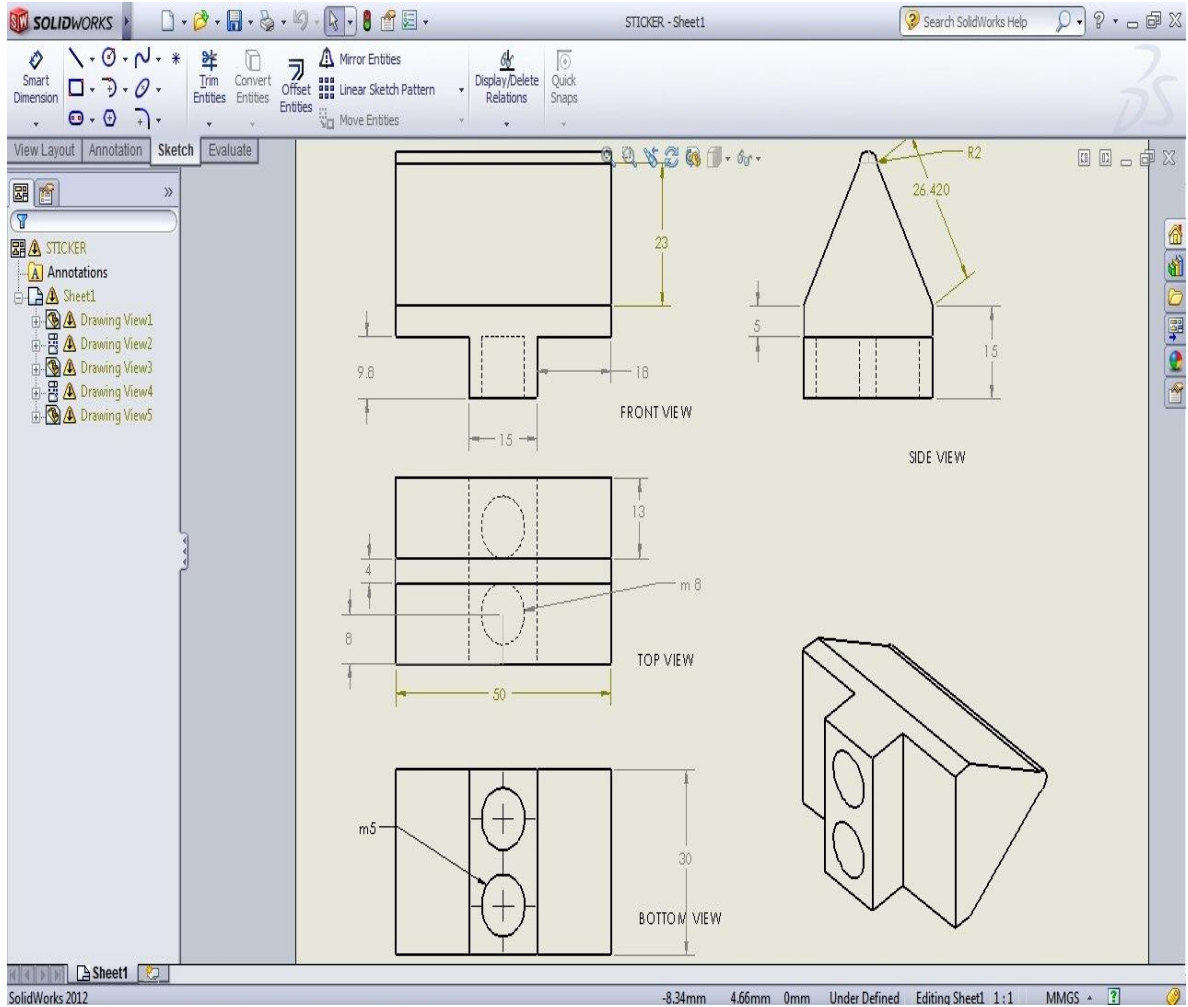


# APPENDIX F

## Beam



# Striker



## Coupling

